DOI:
10.1016/j.mcn.2019.103463

Document Version
Peer reviewed version

Δ^9-tetrahydrocannabinol and 2-AG decreases neurite outgrowth and differentially affects ERK1/2 and Akt signaling in hiPSC-derived cortical neurons.

Carole Shum[1,2], Lucia Dutan[1,2], Emily Annuario[1,2], Katherine Warre-Cornish[1,2], Samuel E. Taylor[2,3], Ruth D. Taylor[2,3], Laura C. Andreae[2,3], Noel J. Buckley[4], Jack Price[1,2,4], Sagnik Bhattacharyya[6]*, Deepak P. Srivastava[1,2]*

[1]Department of Basic and Clinical Neuroscience, The Maurice Wohl Clinical Neuroscience Institute, Institute of Psychiatry Psychology and Neuroscience, King's College London, London, SE5 8AF, UK; [2]MRC Centre for Neurodevelopmental Disorders, King's College London, London, UK; [3]Centre for Developmental Neurobiology, King's College London, London, UK, [4]Department of Psychiatry, University of Oxford, UK; [5]National Institute for Biological Standards and Control, South Mimms, UK [6]Department of Psychosis Studies, King's College London, London, SE5 8AF, UK.

* = corresponding authors: sagnik.2.bhattacharyya@kcl.ac.uk; deepak.srivastava@kcl.ac.uk

Running title: Δ9-THC regulates neurite outgrowth in human neurons

Key Words: Induced pluripotent stem cells, THC, high content screening, human neuron, endocannabinoids, cannabinoid type 1 receptor.

Abstract

Endocannabinoids regulate different aspects of neurodevelopment. *In utero* exposure to the exogenous psychoactive cannabinoid Δ^9-tetrahydrocannabinol (Δ^9-THC), has been linked with abnormal cortical development in animal models. However, much less is known about the actions of endocannabinoids in human neurons. Here we investigated the effect of the endocannabinoid 2-arachidonoyl glycerol (2AG) and Δ^9-THC on the development of neuronal morphology and activation of signaling kinases, in cortical neurons derived from human induced pluripotent stem cells (hiPSCs). Our data indicate that the cannabinoid type 1 receptor (CB1R), but not the cannabinoid 2 receptor (CB2R), GPR55 or TRPV1 receptors, is expressed in young, immature hiPSC-derived cortical neurons. Consistent with previous reports, 2AG and Δ^9-THC negatively regulated neurite outgrowth. Interestingly, acute exposure to both 2AG and Δ^9-THC inhibited phosphorylation of serine/threonine kinase extracellular signal-regulated protein kinases (ERK1/2), whereas Δ^9-THC also reduced phosphorylation of Akt (aka PKB). Moreover, the CB1R inverse agonist SR 141716A attenuated the decrease in neurite outgrowth and ERK1/2 phosphorylation induced by 2AG and Δ^9-THC. Taken together, our data suggest that hiPSC-derived cortical neurons express CB1Rs and are responsive to exogenous cannabinoids. Thus, hiPSC-neurons may represent a good cellular model for investigating the role of the endocannabinoid system in regulating cellular processes in developing human neurons.

Introduction

The endocannabinoid system is a neuromodulatory system with important roles in central nervous system (CNS) development, neuronal function and synaptic plasticity (Gaffuri et al., 2012; Lu and Mackie, 2016). The endocannabinoid system is composed of endogenous cannabinoids, enzymes that synthesize and degrade endogenous cannabinoids and cannabinoid receptors. The cannabinoid 1 receptor (CB1R) is a highly abundant receptor in the CNS, with strong expression in a number of brain regions including the cortex (Lu and Mackie, 2016; Matsuda et al., 1990). Cannabinoid 2 receptor (CB2R) show much lower expression in the CNS, although recent work has shown high inducible expression of CB2Rs under pathological conditions (Miller and Devi, 2011). Several other receptors, such as peroxisome proliferator activated receptors and transient receptor potential channels, are also engaged by cannabinoids (Pertwee et al., 2010).

CB1Rs are members of the superfamily of G protein-coupled receptors that inhibit adenylyl cyclase and activate mitogen-activated protein kinase by signaling through $G_{i/o}$ proteins. Stimulation of CB1R by cannabinoids has been shown to lead to the phosphorylation of serine/threonine kinase Akt and extracellular signal-regulated kinase ERK1/2 (Derkinderen et al., 2003). These kinases may then activate or inhibit their substrates to influence cellular functions such as promoting survival, metabolism and differentiation. Both Akt and ERK1/2 activation have been shown to mediate neurite outgrowth (Wang et al., 2011; Zheng et al., 2008), a key process in neuronal development and plasticity. The primary psychoactive component of cannabis (*Cannabis sativa*), Δ^9-tetrahydrocannabinol (Δ^9-THC) is also thought to act via the CB1R, resulting a wide range of effects including a depression of the

glutamatergic system (Lu and Mackie, 2016). Perturbations in the endocannabinoid system have been implicated in psychiatric disorders such as schizophrenia (Murray et al., 2017). A number of studies have reported a significant association between cannabis use and schizophrenia (Appiah-Kusi et al., 2016; Di Forti et al., 2019; Murray et al., 2017; Pasman et al., 2018). However, a causal link between cannabis use and schizophrenia remains controversial (Murray et al., 2017). It has been argued that there is no evidence that cannabis use triggers psychosis and that the reported effects are due to the individuals already being genetically at risk of schizophrenia (DeLisi, 2008). Conversely, a number of studies have demonstrated that exposure to Δ^9-THC induce psychotic-like symptoms in healthy individuals (Bhattacharyya et al., 2010). Furthermore, in individuals diagnosed with schizophrenia, an acute challenge with Δ^9-THC has been reported to worsen positive symptoms (D'Souza et al., 2005). The consequence of perinatal cannabis exposure has also become of interest, with reports of alter development in off spring in animal models (Tortoriello et al., 2014) and long lasting functional consequences in human and animal models (Scheyer et al., 2019). These controversies highlight the need to better understand the impact that cannabinoids have during human development to better understand the potential detriment effects of perinatal exposure to cannabis.

Much of our knowledge of the endocannabinoid system comes from work using *in vitro* and *in vivo* animal models. It remains unknown how well these data translate to the human neurons. Investigations into the role of endocannabinoids during cortical development have shown that cannabinoids are important axon guidance cues and that endocannabinoid signaling regulates neuronal projection growth and target innervation (Argaw et al., 2011; Berghuis et al., 2007). Furthermore, cannabinoids regulate neuronal morphology through the regulation of small GTPase signaling

pathways and the actin cytoskeleton, resulting in a negative impact on cortical development (Njoo et al., 2015; Roland et al., 2014; Tortoriello et al., 2014). Advances in stem cell technology have enabled the reprogramming of human somatic cells into induced pluripotent stem cells (hiPSCs) (Takahashi et al., 2007; Takahashi and Yamanaka, 2006), which can subsequently be differentiated in to specific neuronal subtypes (Parr et al., 2017). Using this system Guennewig and colleagues demonstrated that exposure of hiPSC-neurons to Δ^9-THC resulted in significant altered expression of genes involved in development, synaptic function, as well as those associated with psychiatric disorders (Guennewig et al., 2018). This supports the use of hiPSCs as a cellular model to investigate the cellular actions of cannabinoids to understand their relevance for health and disease.

In this study, we first examined the expression of cannabinoid receptors during the differentiation of hiPSCs into cortical neurons. Subsequently, we investigated the impact of acute exposure to the endogenous cannabinoid 2-arachidonoyl glycerol (2AG), a full agonist for the CB1R, and Δ^9-THC, a partial agonist for CB1R, on the morphology of young hiPSC-derived cortical neurons. Furthermore, we assessed the ability of 2AG and Δ^9-THC to regulate the activity of ERK1/2 and Akt signaling cascades. Finally, we report that the CB1R inverse agonist SR 141716A (Rimonabant), attenuated the negative regulation of neurite outgrowth and ERK1/2 phosphorylation induced by 2AG and Δ^9-THC. Taken together, our data indicates that CB1Rs are expressed in immature hiPSC-neurons and that 2AG and Δ^9-THC treatment negatively affect neuronal morphology and impact the Akt and ERK1/2 signaling pathways, potentially via CB1R.

Materials and Methods

Reagents

Δ^9-THC (ethanol solution, ab120447) were from Abcam. 2-Arachidonylglycerol (1298), U0126 (1144) and SR 141716A (0923) were from Tocris. Δ^9-THC was prepared by serially diluting the solution in culture media to a 10x stock solution. The CB1R inverse antagonist SR 141716A was dissolved in DMSO and used at a final concentration of 20 nm; an equivalent volume of DMSO or ethanol was used as a vehicle control. A list of antibodies used in this study can be found in **Table 1**.

Human induced pluripotent stem cells (hiPSCs)

HiPSC lines (CTM_01_04, CTM_02_05 and CTM_03_22) were generated from primary keratinocytes as described previously (Cocks et al., 2014) (**Supplementary Figure 1A & B**). Participants were recruited and methods carried out in accordance to the 'Patient iPSCs for Neurodevelopmental Disorders (PiNDs) study' (REC No 13/LO/1218). Informed consent was obtained from all subjects for participation in the PiNDs study. Ethical approval for the PiNDs study was provided by the NHS Research Ethics Committee at the South London and Maudsley (SLaM) NHS R&D Office.

Neuronal differentiation

Neuronal differentiation of hiPSCs was achieved by replacing E8 medium on confluent hiPSCs with neuralization medium: 1:1 mixture of N2- and B27 (Life Technologies) supplemented with 10 μM SB431542 (Sigma-Aldrich) and 1 μM Dorsomorpin (Calbiochem) for dual SMAD inhibition (2i). Cells were maintained at 37°C in normoxic conditions in 2i medium for 7 days with media was replacement every 24 hours. At day 7 the 2i induced neuroepithelial cells were then passaged using

Accutase (Life Technologies) and re-plated at a 1:1 ratio in N2:B27 media without the small molecule inhibitors and supplemented with 10 µM Rock Inhibitor Y-27632 (Sigma Aldrich) until day 12. Cells were then passaged 2 more times following the same procedure described above at days 16 and 20. During neuronal induction, the formation of neural rosettes was evident from approximately day 10 until the differentiation of neural progenitors (NPC) around day 20. NPCs were maintained as mitotic progenitors in neuralization medium supplemented with 10 ng/ml bFGF, 5 µg/ml insulin, 1 mM l-glutamine, 100 µm non-essential amino acids, and 100 µM 2-mercaptoethanol. NPC were terminally plated on 5 µg/ml poly-D-lysine and 2 µg/cm^2 laminin (Thermo Fisher) in B27 medium supplemented with 200 µM L-ascorbic acid and 10 µM DAPT (Calbiochem) for 7 days (day 27) to block NOTCH signaling. Neurons were grown in B27 medium with 200 µM L-ascorbic acid until day 30 when they were used for experimentation.

Treatments

Acute pharmacological treatment (15 or 30 minutes) of cells was performed in ACSF solution (125 mM NaCl, 2.5 mM KCl, 26.2 mM $NaHCO_3$, 20 mM glucose, 5 mM Hepes, 2.5 mM $CaCl_2$ and 1.25 mM $MgCl_2$). Prolonged pharmacological treatment (24 hour) was performed in Neurobasal medium supplemented with B27 and 200 µM L-ascorbic acid.

qRT-PCR

Total RNA harvested and lysed with Trizol reagent (Life technologies) and isolated by centrifugation with 100% Chloroform, following by 100% isopropanol and lastly by 75% ethanol. The RNA was purified by precipitation with 100% ethanol and

Sodium acetate (Life technologies) and quantify with the NanoDrop 1000 Spectrophotometer (Thermo scientific). Residual genomic DNA was removed by addition of TURBO DNA-free (Life technologies) and incubation at 37°C for 30 minutes. Complementary DNA (cDNA) was synthesized from 1 µg of total RNA from each extraction using random hexamer primers and SuperScript III (Life Technologies) following the manufacturer's recommendations. qPCR was performed with HOT FIREPol EvaGreen qPCR Mix Plus ROX (Solis Biodyne) carried out according to the manufacturer's instructions in a total volume of 20 µl, containing 1:5 diluted cDNA, qPCR mix and primers at to a final concentration of 0.3 µM. PCR reaction conditions: 95^{o}C for 15 minutes for the initial denaturation followed by 95^{o}C for 30 seconds, 60^{o}C for 30 seconds and 72^{o}C for 30 seconds during 33 cycles. The melting curve analyses was preformed from 60^{o}C to 95^{o}C with readings every 1^{o}C. The 2^ Δ Δ CT comparative method for relative quantification was used to quantify the genes expression. The data CT values were normalized to GAPDH, RPL27 and SDHA housekeeping genes.

Immunocytochemistry

Treated neurons were fixed with 4% formaldehyde plus 4% sucrose in PBS. Fixed neurons were permeabilized in 0.1% Triton-X-100 in PBS for 15 minutes and blocked in 4% normal goat serum in PBS for 1 hour at room temperature. Primary antibodies were added to the block solution in an antibody dependent concentration and incubated overnight at 4°C. Immunoreactivity was achieved by incubating the cells with 1:500 concentration of Alexa Fluor 594 conjugated anti-mouse IgG, Alexa Fluor 594 conjugated anti-goat IgG and Alexa Fluor 488 conjugated anti-rabbit IgG in block buffer. For nuclei staining a 1:2000 concentration of DAPI (Thermo Fisher) was used.

Imaging of immunofluorescence by high content image screening

NPCs were plated at a density of $1x10^4$ cells/well on poly-D-lysine and laminin-coated optical-bottom 96 well plates with polymer base (ThermoScientific). Image acquisition was performed with a 20X objective for the genes OCT4, NANOG, SOX11, ZNF521, PAX6, NESTIN, FOXG1, TBR1, TBR2 and BRN1 by using CellInsight CX5 High Content Screen Platform (Thermo Fisher). The bioapplication Cell Health Profiling from the iDev software package (Thermo Fisher) using the nuclear staining to assess viable cells. Intensity, shape and size features were used to determine positively labelled cells.

For neurite outgrowth assays, treated hiPSC-neurons were imaged using an Opera Phenix High Content screening platform (Perkin Elmer): images were acquired using a 20 x (NA 0.4) objective. The Harmony High Content Imaging and Analysis Software was used to determine the average neurite length and average branch number based on the MAP2 staining. For each hiPSC line, 3 biological replicates with 3 technical replicates per condition were imaged and analyzed: 15 randomly selected fields from each technical replicate was examined. Data from each technical replicate was averaged and used as a single data point and compared with each biological replicate and each hiPSC line. The means of percentages of positive cells and the average neurite length and branch number were compared by an ANOVA. Confocal images of hiPSC-neurons stained for MAP2 and CB1R were acquired using a Lecia SP5 confocal microscope using a 63x oil objective (NA 1.4) as a z-series. Post image acquisition, images were z-projected using ImageJ (rsb.info.nih.gov/ij/).

Western blotting

hiPSC-neurons cells were lysed in 20 mM Tris, pH 7.2, 150 mM NaCl, 1% Triton-X-100, 5 mM EDTA pH 8 containing a cocktail of protease and phosphatase inhibitors (1mg/ml leupeptin, 5mg/ml aprotinin, 1M NaF, 1mg/ml pepstatin, 100mM AEBSF, and Ser/Thr phosphatase inhibitor cocktail #3). Detergent soluble lysate were resolved by SDS-PAGE, then immunoblotted with primary antibodies overnight at 4°C, followed by incubation with anti-mouse Alexa Fluor 680 and anti-rabbit Alexa Fluor 790 IgG (H+L) secondary antibodies for 1 hour at room temperature. Membranes were scanned with Odyssey imaging system (LI-COR). Intensities of bands were quantified by densitometry using Image J (rsb.info.nih.gov/ij/). Full length blots are shown in Supplemental Figures 3, 5, 6 and 7**.**

Statistical analysis

All statistical analysis was performed in GraphPad. Differences in 2^ Δ Δ CT, relative expression, cell number and neurite parameters were identified by Student's unpaired t-tests, or for comparisons between multiple conditions the main effects and simple effects were probed by one-way-ANOVAs or two-way-ANOVAs with Tukey or Bonferroni correction for multiple comparisons. Differences were considered significant if *P* was lower than 0.05 ($p < 0.05$). Error bars represent standard errors of the mean unless stated otherwise.

Results

Generation of cortical neurons from hiPSCs

Within the developing CNS, the endocannabinoid system has been implicated in important neuronal processes such as synapse formation and neurogenesis (Gaffuri

et al., 2012; Lu and Mackie, 2016). CB1Rs are G-protein coupled receptors that are widely expressed in the brain (Matsuda et al., 1990), including the cortex (Gaffuri et al., 2012; Lu and Mackie, 2016). Consistent with a role for the endocannabinoid system during the development of cortical neurons, acute (24 hour) exposure of hiPSC-neurons to Δ^9-THC results in the differential expression of multiple genes, including those involved in development (Guennewig et al., 2018). Therefore, in order to further understand the role of cannabinoids during the development of human cortical neurons, we induced cortical differentiation from hiPSC. The cell lines were derived by reprogramming keratinocytes from 3 neurotypic males (age ranging between 35 to 55 years: CTM_01_04, CTM_02_05 and CTM_03_22; **Supplementary Figure 1A and B**) (Cocks et al., 2014; Deans et al., 2017; Kathuria et al., 2018; Shum et al., 2015). HiPSC lines were differentiated into neuroepithelial cell using a dual SMAD inhibition (2i) differentiation protocol for 8 days (Cocks et al., 2014; Deans et al., 2017; Shum et al., 2015) (**Figure 1A**). The small molecule inhibitors were removed during neuronal progenitor's differentiation before media was replaced with B27 supplemented with DAPT to induce the generation of terminally differentiated neurons (Cocks et al., 2014; Deans et al., 2017; Shum et al., 2015) (**Figure 1A**). Immunocytochemical (ICC) analyses indicated that the derived hiPSC expressed high levels of the pluripotency markers OCT4, NANOG and SOX11, whereas early neural progenitor cell (NPC) markers PAX6, ZNF521 and NESTIN were up regulated following 8 days of 2i induction (**Figure 1B and 1C**). After 26 days of neuronal differentiation young neurons expressed high levels of the transcription factors FOXG1, TBR1 and TBR2, which are required for the differentiation of cortical neurons (**Figure 1B and 1C**). Similarly, real time PCR (qPCR) analyses demonstrated that the neuroepithelial marker SOX2 was highly expressed 7 days after 2i induction and was

gradually down-regulated during the 50 days of neuronal fate acquisition (**Figure 1D**). PAX6, a key regulator of cortical development, was found to be highly expressed from day 7 to day 50 during neuronal formation; peak expression was observed at day 22 (**Figure 1E**). The expression of CTIP2, a marker of deep layer cortical cell fate, rapidly increased from day 24 to day 30, peaking at day 26; subsequently, expression of CTIP2 was down-regulated until day 50 (**Figure 1F**). Conversely, expression of BRN2, a marker associated with upper cortical layer cell fate, showed expression peaks at days 23, 26 and once more at day 40 (**Figure 1G**). At day 30, few or no GFAP or S100β positive cells were observed (**Supplementary Figure 2A**). ICC analysis at day 50 revealed that most MAP-positive cells were also immunoreactive for markers of glutamatergic fate. This included the pre-synaptic proteins synapsin 1 and VGlut1 and the post-synaptic proteins PSD95 and GluN1-subunit of NMDA receptors (**Supplementary Figure 2B-D**). To confirm that hiPSC-neurons generated from a hiPSC line derived from keratinocytes, and following our 2i cortical protocol, develop physiological neuronal characteristics as previously described (Kathuria et al., 2018; Shi et al., 2012), we conducted whole-cell patch clamp recordings in hiPSC-neurons differentiated for 64 days. Current clamp recordings demonstrated that these cells were capable of firing an action potential in response to current injection (**Supplementary Figure 2E**). Depolarising step potentials (from a holding potential of -60mV) evoked transient inward currents and sustained outward currents, indicative of activation of voltage gated sodium channels and potassium channels respectively (**Supplementary Figure 2F**). At this age, we were able to record isolated spontaneous excitatory postsynaptic currents (EPSCs), demonstrating the potential presence of functional excitatory synaptic connections at this stage (**Supplementary Figure 2G**). These data are consistent with previous studies indicating that hiPSC-neurons

generated using the 2i protocol develop physiological characteristics; however, the remaining data in this study were produced using hiPSC-neurons at an earlier developmental stage.

CB1R expression during the cortical differentiation of iPSCs

Previous studies have suggested that CB1Rs are highly expressed during neuronal development (Lu and Mackie, 2016). Therefore, we examined the expression of *CB1R* mRNA in hiPSC-derived NPCs and terminally differentiated neurons. In all three hiPSC lines, *CB1R* showed similar expression patterns. Specifically, *CB1R* mRNA levels significantly increased as hiPSCs differentiated from NPCs into neurons (**Figure 2A**). We further examined the expression of enzymes involved in endocannabinoid synthesis and metabolism. Expression of *DAGLA* increased as cells differentiate into neurons (**Supplementary Figure 3A)**. Interestingly, both *FAAH* and *MGLL* were expressed at similar levels in both NPC and neurons (**Supplementary Figure 3A)**. We also examined the expression of *CB2R*, *GPR55* and *TRPV1* receptors which are expressed in the brain and are engaged by cannabinoids in differentiated neurons (Gaffuri et al., 2012; Lu and Mackie, 2016). The mRNA expression levels of these receptors were mirrored across the three hiPSC lines and was significantly lower compared with the expression of *CB1R* (**Figure 2B**). Next, we examined the expression of CB1R protein in immature hiPSC-neurons using an antibody raised against the C-terminal of the receptor; this antibody has been validated in knockout tissue and human tissue (Bjorklund et al., 2011; Chung et al., 2009) as well by pre-absorption studies (**Supplemental Figure 3B**). Western blotting demonstrated that the receptor was expressed at the protein level in immature hiPSC-neurons. A prominent band ~53 kDa consistent with the predicted molecular weight for the

receptor, was readily observed (**Figure 2C; Supplemental Figure 3C**). Consistent with these data, immunostaining of immature hiPSC-neurons revealed that CB1R staining could be observed in all three hiPSC clonal lines. CB1R immunoreactivity could be observed as in punctate structures along MAP2-positive neurites (**Figure 2D**). Collectivity, these data demonstrate that CB1Rs are expressed in immature hiPSC-neurons.

2AG and Δ^9-THC decrease neurite outgrowth in hiPSC-neurons.

There is growing appreciation that the endocannabinoid system is an important regulator of brain wiring during development through the modulation of several different processes including the specification of neuronal morphology (Njoo et al., 2015; Roland et al., 2014; Vitalis et al., 2008; Watson et al., 2008; Wu et al., 2010). As CB1Rs are localized along the neurite, we reasoned that endocannabinoids may be involved in regulating the establishment of neuronal morphology in hiPSC-neurons. To test this prediction, we first treated hiPSC-neurons at day 29 with 1 µM 2AG, a full agonist for the CB1R, for 24 hours. Neurons were then fixed and stained for MAP2 to outline neuronal morphology. Neurite outgrowth was assayed using a high-content screening platform (**Figure 3A**). We first assessed whether treatment with 2AG altered the number of MAP2-positive cells; this revealed no differences between conditions in neurons derived from all 3 hiPSC lines (**Figure 3B**; p=0.931). We next examined neuronal morphology and demonstrated that the average number of neurites (**Figure 3C**; p=0.713) and number of branch points (**Figure 3D**; p=0.780) were unaffected by treatment in neurons derived from all 3 hiPSC lines. However, 2AG treatment for 24 hours significantly reduced neurite length (**Figure 3E**; $F(1,18)=23.4$, $p < 0.001$, Bonferroni Post Hoc, * $p < 0.05$; two-way ANOVA; n = 3 independent cultures per

hiPSC line) in neurons derived from all 3 hiPSC lines. Interestingly, a lower concentration (50 nM) of 2AG did not significantly alter neurite length in all 3 hiPSC-lines (**Supplemental Figure 4A**; P=0.475).

Δ^9-THC has previously been shown to negatively regulate neurite outgrowth and growth cone dynamics, through the regulation of actin polymerization and microtubule stability in mouse cortical neurons (Njoo et al., 2015; Tortoriello et al., 2014; Vitalis et al., 2008). In addition, exposure to Δ^9-THC in hiPSC-neurons results in the altered expression of multiple genes involved in the development of neuronal morphology (Guennewig et al., 2018). Therefore, we next examined whether acute exposure to Δ^9-THC could also alter neurite outgrowth. D29 hiPSC-neurons were treated with 3 µM Δ^9-THC for 24 hours before neuronal morphology was examined using a high-content screening platform (**Figure 4A**). Δ^9-THC treatment did not significantly affect the number of MAP2-postive cells across the three hiPSC-lines (**Figure 4B**; p=0.647). Similar to 2AG, exposure to Δ^9-THC did not significantly alter neurite number (**Figure 4C**; p=0.426) or branch points (**Figure 4D**; p=0.859). However, Δ^9-THC treatment for 24 hours significantly reduced the neurite length (**Figure 4E**; $F(1,18)=26.05$, $p < 0.001$, Bonferroni Post Hoc, * $p < 0.05$; two-way ANOVA; n = 3 independent cultures per hiPSC line) in neurons derived from all 3 hiPSC lines. A lower concentration of Δ^9-THC (50 nM) had no effect on neurite length in all 3 hiPSC-lines (**Supplemental Figure 4B**; P=0.266). Taken together, these data indicate that both 2AG and Δ^9-THC decreases neurite outgrowth in young hiPSC-neurons.

2AG and Δ^9-THC modulate phosphorylation of serine/threonine kinases Akt and mitogen-activated protein kinase ERK1/2.

Stimulation of CB1R leads to the phosphorylation and activation of several signaling kinases, including Akt, ERK1/2 and GSK3β (Derkinderen et al., 2003; Gaffuri et al., 2012; Ozaita et al., 2007). Akt and ERK1/2 pathways have also been implicated in promoting neurite outgrowth(Wang et al., 2011),(Zheng et al., 2008). GSK-3β, a well-defined substrate of Akt, has also been implicated in the regulation of neurite and axonal outgrowth and branching (Namekata et al., 2012). Interestingly, the negative effects of CB1R activation on neurite outgrowth have been linked with ERK1/2 signaling (Guennewig et al., 2018), although activation of CB1R has also been linked with Akt and GSK3β signaling *in vivo* (Ozaita et al., 2007). Therefore, we first examined 2AG generated changes in the activation state (phosphorylation) of ERK1/2, Akt and GSK3β kinases in day 30 hiPSC-neurons. Remarkably, 2AG treatment resulted in a significant decrease in ERK1/2 phosphorylation after 30 minutes (**Figure 5A)**. Conversely, no changes in the phosphorylation state of Akt or GSK3β were detected following 15 and 30 minutes of 2AG exposure (**Figure 5B and C**). These data demonstrated that 2AG, a full agonist for the CB1R, is capable of decreasing ERK1/2 activity.

Owing to our data demonstrating that 2AG negatively regulated ERK1/2 phosphorylation, we next investigated the effect of Δ^9-THC on ERK1/2, Akt and GSK3β kinases. D30 hiPSC-neurons were treated with vehicle or 3 μM Δ^9-THC for either 15 or 30 minutes. Similar to 2AG treatment, Δ^9-THC induced a rapid decrease in ERK1/2 phosphorylation (**Figure 5D)**. Interestingly, Δ^9-THC also caused a rapid reduction in levels of phosphorylated Akt, which was evident after 15 minutes (**Figure 5E)**. No change in phosphorylated GSK3β was observed following Δ^9-THC treatment (**Figure 5F**). Collectively, these data indicate that Δ^9-THC decreases both ERK1/2 and Akt phosphorylation, in contrast to 2AG, which regulates ERK1/2 exclusively.

2AG and Δ^9-THC modulation of kinase activity and neurite outgrowth is blocked by CB1R receptor antagonism.

As our data indicated that 2AG negatively regulated ERK1/2 and that Δ^9-THC decreased the activity of both ERK1/2 and Akt signaling kinases, we were interested in understanding whether these effects were being mediated by the CB1R. Recently, Obiorah et al. showed that Δ^9-THC mediated changes in glutamate receptor gene expression in hiPSC-neurons could be blocked using the CB1R selective inverse antagonist SR 141716A (Rimonabant) (Obiorah et al., 2017). Pre-treatment with 20 nM SR 141716A blocked 2AG and Δ^9-THC (30 minutes) induced de-phosphorylation of ERK1/2; SR 141716A alone had not effect on pERK1/2 levels (**Figure 6A**; $F(1.309,2.618)=12.07$, $p = 0.0489$, Tukey Post Hoc, * $p < 0.05$; one-way ANOVA). As previously seen, Δ^9-THC, but not 2AG (30 minutes) caused a reduction in pAkt levels. This effect was blocked by pre-treatment with 20 nM SR 141716A (**Figure 6B**; $F(1.542,3.083)=14.15$, $p = 0.0291$, Tukey Post Hoc, * $p < 0.05$; one-way ANOVA).

As our data indicated that the CB1R mediates the effects of 2AG and Δ^9-THC on ERK1/2 activity, we next questioned whether this receptor was required for the decrease in neurite outgrowth induced by these cannabinoids. To test this, we treated day 29 hiPSC-neurons with 2AG or Δ^9-THC with or without SR 141716A. Treatment with 2AG or Δ^9-THC caused a reduction in total neurite length; this was attenuated by co-treatment with SR 141716A (**Figure 7A and B**; $F(2,36)=6.524$, $p=0.0038$, Bonferroni Post Hoc, * $p < 0.05$, ** $p < 0.01$, *** $p < 0.001$; two-way ANOVA; $n = 3$ independent cultures per hiPSC line). Next, we reasoned that if 2AG or Δ^9-THC were causing a reduction in neurite outgrowth by negatively regulating the ERK1/2 pathway, that inhibiting this kinase pathway would mimic the effects of these cannabinoids on

neurite outgrowth. Therefore, we treated day 29 hiPSC-neurons with 10 μM U0126, a MEK inhibitor. Assessment of neurite outgrowth on day 30 revealed that neurons treated with U0126 had reduced total neurite length (**Supplementary Figure 8A and B**; $F(1,8)=24.1$, $p=0.0012$, Bonferroni Post Hoc, * $p < 0.05$; two-way ANOVA; n = 3 independent cultures per hiPSC line). Taken together, these data indicate that antagonism of the CB1R by SR 141716A or is sufficient to attenuate the negative effects of 2AG and Δ^9-THC on kinase activity and neurite outgrowth.

Discussion

Recently it has been demonstrated that cannabinoid treatment affects neuronal function and glutamate receptor expression in hiPSC-derived dopaminergic neurons and excitatory neurons, respectively (Obiorah et al., 2017; Stanslowsky et al., 2017). Moreover, treatment with Δ^9-THC induces a wide range of transcriptional changes in cortical hiPSC-neurons. This includes changes in the expression of genes involved in neurodevelopmental processes, as well as those associated with neurodevelopmental and psychiatric disorders (Guennewig et al., 2018). Despite this, it is not clear what role the endocannabinoid system plays during neurodevelopment. In this study, we demonstrate that the CB1R is the major cannabinoid receptor expressed during early differentiation of cortical hiPSC-neurons. Furthermore, we demonstrate that treatment with either 2AG or Δ^9-THC decreased neurite outgrowth, as well as differential effects on the activation status of ERK1/2 and Akt signaling kinases. Furthermore, the effect of 2AG and Δ^9-THC on kinase activity and neurite outgrowth could be blocked by the CB1R inverse agonist SR 141716A, potentially implicating the CB1R receptor in these effects.

Previously, Stanslowsky et al. (2017) observed an upregulation of *CB1R* mRNA following terminal differentiation of hiPSC-derived dopaminergic neurons and the predominant expression of CB1R in hiPSC-derived neural precursors(Stanslowsky et al., 2017). CB1R has also been reported to be highly expressed in newly differentiated glutamatergic neurons and is labelled in a punctate manner in the soma and neurites of these cells suggesting a prominent role for this receptor during this developmental time point (Vitalis et al., 2008). In agreement with these reports, we observed that *CB1R* mRNA is differentially up-regulated during neuronal differentiation in three hiPSC lines with different genetic background. Moreover, at the protein level, we observed CB1R to be expressed in immature hiPSC-derived cortical neurons, where it localized in the cell soma and along neurites. Furthermore, we found that hiPSC-derived glutamatergic-neurons expressed *CB1R* mRNA at significantly higher levels compared to *CB2R*, *GPR55* and *TRPV1*. These findings provide support for the idea that the CB1R may play an important role in early neurodevelopmental processes such as progenitor cell differentiation and neurite outgrowth, prior to the formation of synapses.

The impact of perinatal exposure to cannabis has come to attention of recent (Scheyer et al., 2019). In animals and humans Δ^9-THC rapidly crosses the placenta. The concentrations of Δ^9-THC in fetal blood closely approximates that in maternal blood. Blood and plasma Δ^9-THC levels after smoking or vaporizing cannabis have been reported to range from 1.6-210 µg/L, or about 5-667 nM (Hartman et al., 2016; Marsot et al., 2016). The concentration of Δ^9-THC used in this study is similar to previous studies of *in vitro* and *in vivo* animal models, but higher than that reported in blood and plasma after smoking or vaporizing cannabis. It should be noted that these studies were performed on male participants, and it is unclear whether sex differences

exist in the pharmacokinetics of Δ^9-THC and its metabolites. Studies on the effect of cannabinoids on neurite outgrowth have been attempted with various CB1R agonists and have produced conflicting results (Gaffuri et al., 2012). Whereas Δ^9-THC treatment in murine dopaminergic neurons had no effect on morphology (Moldzio et al., 2012), Δ^9-THC treatment reduced neurite length in primary neurons from E16.5 mouse cortices (Tortoriello et al., 2014). Similarly, activation of CB1R by HU210 has been shown to trigger neurite outgrowth in Neuro2A cells (Zorina et al., 2010), while CB1R agonist WIN55,212-2 negatively regulates dendritic and axonal outgrowth in cultured rat hippocampal neurons (Vitalis et al., 2008). We investigated the effects of the endogenous cannabinoid 2AG and the exogenous cannabinoid Δ^9-THC on neuronal morphology. In our study, we observed that both 2AG and Δ^9-THC decreased total neurite outgrowth in hiPSC-derived glutamatergic neurons. Vitalis et al. (2008) previously showed that basal activation of CB1R acts as a negative regulatory signal for neuritogenesis, and treatment with inverse agonist AM281 blocked these effects (Vitalis et al., 2008). Argaw et al. (2011) showed that pharmacological treatment with ACEA, a selective CB1R agonist, induced a collapse of the growth cone, an important structure for axon pathfinding and neurite outgrowth. Conversely, treatment with AM251, a CB1R inverse agonist, increased the surface of the growth cone. These findings establish a mechanism through which the CB1R affects growth cone structure in the development of the visual system. The high content imaging platform used in this study precluded an accurate measurement of growth cone size; however, further investigation of the growth cone in hiPSC-neurons would provide greater insight of the mechanisms through which cannabinoids may regulate neuronal morphology in developing human neurons. Changes in neuronal morphology are believed to be related to changes in neuronal function, as different

neuronal subtypes vary in the number and amount of axonal and dendritic branches and outgrowth. Migrating cortical projection neurons initially have a bipolar morphology in the ventricular zone, then transition to a multipolar morphology in the subventricular zone or intermediate zone, where cells extend and retract processes dynamically, eventually extending an axon prior to resuming radial migration and transforming back to a bipolar cell morphology and entering the cortical plate (Tabata and Nakajima, 2003). Using the developing visual system as a model, Argaw et al. (2011) showed that intraocular injection of ACEA induced a decrease in retinal ganglion cell axon growth *in vivo,* whereas intraocular injection of AM251 increased retinal ganglion cell collateral length and branch number (Argaw et al., 2011). In this study, the reduced total neurite length as a result of cannabinoid treatment suggests a possible dysregulation of neuronal projection growth, which could influence the differentiation and maturation of hiPSCs into functional cortical neurons. Future examination of axon growth would be important as 2AG/Δ^9-THC could impact axon guidance differently. It is of note that whilst we demonstrate that exogenous application of 2AG or Δ^9-THC alters neurite outgrowth, this does not definitively show that the endocannabinoids in involved in this process in hiPSC-neurons. Future studies where CB1R is directly antagonized or genetically knocked out would clarify this point. Nevertheless, data from previous studies as well as those presented in this study suggest that endocannabinoids may regulate neuronal morphology in developing neurons. However, the specific downstream mechanisms underlying this process are not well-described, and further research is required to delineate how different cannabinoids affect neuritogenesis in growing and mature neurons, from humans and other animal species.

CB1R signaling is a complex process and cannabinoids can phosphorylate and activate members of all three families of multifunctional mitogen-activated protein kinases, as well as the PI3K/Akt pathway (Howlett, 2005; Sanchez et al., 2003). We examined the signal transduction pathways regulated by the activation of CB1Rs, focusing on the effect of 2AG and Δ^9-THC on the Akt and ERK1/2 pathways. Studies on the effect of cannabinoids on these pathways have been attempted with various CB1R agonists and have produced conflicting results. Several studies of non-neuronal cells and hippocampal slices and hippocampal neurons in living mice previously demonstrated that stimulation of CB1Rs by endocannabinoids anandamide, 2AG and exogenous Δ^9-THC activates ERK1/2 (Bouaboula et al., 1995; Derkinderen et al., 2003), whereas stimulation of CB1R by selective CB1R agonist ACEA in primary cortical neurons did not alter the phosphorylation of ERK1/2 or Akt (Argaw et al., 2011). In contrast, an increase in the phosphorylation of Akt and of GSK3β by acute Δ^9-THC, anandamide and HU-210 administration has been demonstrated *in vivo* (Kokona and Thermos, 2015; Ozaita et al., 2007). In this study, 2AG did not affect the phosphorylation and activation of Akt, whereas Δ^9-THC reduced the levels of phosphorylated Akt. Furthermore, both cannabinoids reduced the levels of phosphorylated ERK1/2. These effects were attenuated by co-treatment with SR 141716A, suggesting that they are mediated by the CB1R. Interestingly, application of SR141716A alone had no effect on the levels of phosphorylated ERK1/2 or Akt. Previous studies have shown that SR141716A can exhibit either an inverse agonism or an apparent neutral competitive antagonism, depending on the assay system. For instance, cannabinoid agonists mediated the inhibition of depolarization-induced epinephrine release from hippocampal slices, an effect that was antagonized by SR141716A (Schlicker et al., 1997), but when administered alone, SR141716A had

no effect on the stimulated release of norepinephrine from human hippocampal slices (Selley et al., 1996). Our observations suggest that in hiPSC-neuronal cultures, SR141617A may have no activity in the absence of an agonist or inverse agonist, but can block the activity of either. Overall, previous data and ours suggest that both endogenous and exogenous cannabinoids affect the ERK1/2 and Akt signaling pathways. It is possible that in different model systems, CB1R activation triggers different signaling pathways to regulate downstream gene expression and neuronal processes. The specific pharmacology of CB1R signaling is not well understood, and further research is necessary to describe how endogenous, exogenous and synthetic cannabinoids act on CB1R and how they may or may not interact to trigger or inhibit downstream signaling pathways. One possibility is that owing to the repertoire of signaling proteins that are expressed in these developing neurons, that 2AG and Δ^9-THC couple the CB1R to the negative regulation of these kinases via a mechanism known as biased receptor signaling (Kenakin, 2019).

Overall, the results of the present study suggest that exogenous 2AG and Δ^9-THC are able to induce morphological changes in young hiPSC-derived glutamatergic neurons, further supporting the notion that this cellular system is a good model for investigating cannabinoid function in early development (Guennewig et al., 2018). A recent study showed that pluripotent stem cells derived from males and females display more than 200 differentially expressed autosomal genes (Ronen and Benvenisty, 2014). In addition, sex differences in neuronal morphology have been reported in hiPSC-neurons in a model of traumatic axonal injury (Dolle et al., 2018). This proof-of-concept study has demonstrated that male hiPSC-neurons are responsive to pharmacological manipulation of the cannabinoid system. Future studies using hiPSC-neurons derived from neurotypical females would allow an

examination of potential sex differences in neuronal development and responses to cannabinoids.

CB1Rs were first identified as the main neuronal receptor for Δ^9-THC and are one of the most abundant G protein-coupled receptors in the brain(Matsuda et al., 1990). CB1Rs and endocannabinoids are also highly expressed in the fetal brain and implicated in neuronal development processes such as neurite growth and axonal pathfinding (Njoo et al., 2015; Tortoriello et al., 2014; Vitalis et al., 2008; Watson et al., 2008; Wu et al., 2010; Zorina et al., 2010). In this present study, we have examined the endocannabinoid 2-AG and its effects in hiPSC-neurons. Anandamide is another endocannabinoid that is also present during development. Future studies using a wider range of CB receptor-specific agonists would provide a deeper understanding of the pharmacology underlying eCB signaling in hiPSC-neurons. We show that exogenous cannabinoids modulate neurite outgrowth in hiPSC-neurons, and previous studies have shown that endogenous and exogenous cannabinoids alter synaptic activity and synaptic protein expression in developing human hiPSC-derived neurons (Obiorah et al., 2017; Stanslowsky et al., 2017). Moreover, as Δ^9-THC has recently been shown to alter expression of genes associated with neurodevelopmental and psychiatric disorders, there is evidence for perturbations of shared molecular pathways potentially exacerbated by Δ^9-THC (Guennewig et al., 2018). Whether or not overstimulation by exogenous cannabinoids or abnormal levels of endocannabinoids during neurodevelopment may perturb normal physiological processes, potentially contributing to neurodevelopmental and psychiatric disorders will require further in-depth studies in the future.

References

Appiah-Kusi, E., Leyden, E., Parmar, S., Mondelli, V., McGuire, P., Bhattacharyya, S., 2016. Abnormalities in neuroendocrine stress response in psychosis: the role of endocannabinoids. Psychol Med 46, 27-45.

Argaw, A., Duff, G., Zabouri, N., Cecyre, B., Chaine, N., Cherif, H., Tea, N., Lutz, B., Ptito, M., Bouchard, J.F., 2011. Concerted action of CB1 cannabinoid receptor and deleted in colorectal cancer in axon guidance. J Neurosci 31, 1489-1499.

Berghuis, P., Rajnicek, A.M., Morozov, Y.M., Ross, R.A., Mulder, J., Urban, G.M., Monory, K., Marsicano, G., Matteoli, M., Canty, A., Irving, A.J., Katona, I., Yanagawa, Y., Rakic, P., Lutz, B., Mackie, K., Harkany, T., 2007. Hardwiring the brain: endocannabinoids shape neuronal connectivity. Science 316, 1212-1216.

Bhattacharyya, S., Morrison, P.D., Fusar-Poli, P., Martin-Santos, R., Borgwardt, S., Winton-Brown, T., Nosarti, C., CM, O.C., Seal, M., Allen, P., Mehta, M.A., Stone, J.M., Tunstall, N., Giampietro, V., Kapur, S., Murray, R.M., Zuardi, A.W., Crippa, J.A., Atakan, Z., McGuire, P.K., 2010. Opposite effects of delta-9-tetrahydrocannabinol and cannabidiol on human brain function and psychopathology. Neuropsychopharmacology 35, 764-774.

Bjorklund, E., Forsgren, S., Alfredson, H., Fowler, C.J., 2011. Increased expression of cannabinoid CB(1) receptors in Achilles tendinosis. PLoS One 6, e24731.

Bouaboula, M., Poinot-Chazel, C., Bourrie, B., Canat, X., Calandra, B., Rinaldi-Carmona, M., Le Fur, G., Casellas, P., 1995. Activation of mitogen-activated protein kinases by stimulation of the central cannabinoid receptor CB1. Biochem J 312 (Pt 2), 637-641.

Chung, S.C., Hammarsten, P., Josefsson, A., Stattin, P., Granfors, T., Egevad, L., Mancini, G., Lutz, B., Bergh, A., Fowler, C.J., 2009. A high cannabinoid CB(1) receptor

immunoreactivity is associated with disease severity and outcome in prostate cancer. Eur J Cancer 45, 174-182.

Cocks, G., Curran, S., Gami, P., Uwanogho, D., Jeffries, A.R., Kathuria, A., Lucchesi, W., Wood, V., Dixon, R., Ogilvie, C., Steckler, T., Price, J., 2014. The utility of patient specific induced pluripotent stem cells for the modelling of Autistic Spectrum Disorders. Psychopharmacology (Berl) 231, 1079-1088.

D'Souza, D.C., Abi-Saab, W.M., Madonick, S., Forselius-Bielen, K., Doersch, A., Braley, G., Gueorguieva, R., Cooper, T.B., Krystal, J.H., 2005. Delta-9-tetrahydrocannabinol effects in schizophrenia: implications for cognition, psychosis, and addiction. Biol Psychiatry 57, 594-608.

Deans, P.J.M., Raval, P., Sellers, K.J., Gatford, N.J.F., Halai, S., Duarte, R.R.R., Shum, C., Warre-Cornish, K., Kaplun, V.E., Cocks, G., Hill, M., Bray, N.J., Price, J., Srivastava, D.P., 2017. Psychosis Risk Candidate ZNF804A Localizes to Synapses and Regulates Neurite Formation and Dendritic Spine Structure. Biol Psychiatry 82, 49-61.

DeLisi, L.E., 2008. The effect of cannabis on the brain: can it cause brain anomalies that lead to increased risk for schizophrenia? Curr Opin Psychiatry 21, 140-150.

Derkinderen, P., Valjent, E., Toutant, M., Corvol, J.-C., Enslen, H., Ledent, C., Trzaskos, J., Caboche, J., Girault, J.-A., 2003. Regulation of Extracellular Signal-Regulated Kinase by Cannabinoids in Hippocampus. The Journal of Neuroscience 23, 2371-2382.

Di Forti, M., Quattrone, D., Freeman, T.P., Tripoli, G., Gayer-Anderson, C., Quigley, H., Rodriguez, V., Jongsma, H.E., Ferraro, L., La Cascia, C., La Barbera, D., Tarricone, I., Berardi, D., Szoke, A., Arango, C., Tortelli, A., Velthorst, E., Bernardo, M., Del-Ben, C.M., Menezes, P.R., Selten, J.P., Jones, P.B., Kirkbride, J.B., Rutten,

B.P., de Haan, L., Sham, P.C., van Os, J., Lewis, C.M., Lynskey, M., Morgan, C., Murray, R.M., Group, E.-G.W., 2019. The contribution of cannabis use to variation in the incidence of psychotic disorder across Europe (EU-GEI): a multicentre case-control study. Lancet Psychiatry 6, 427-436.

Dolle, J.P., Jaye, A., Anderson, S.A., Ahmadzadeh, H., Shenoy, V.B., Smith, D.H., 2018. Newfound sex differences in axonal structure underlie differential outcomes from in vitro traumatic axonal injury. Exp Neurol 300, 121-134.

Gaffuri, A.L., Ladarre, D., Lenkei, Z., 2012. Type-1 cannabinoid receptor signaling in neuronal development. Pharmacology 90, 19-39.

Guennewig, B., Bitar, M., Obiorah, I., Hanks, J., O'Brien, E.A., Kaczorowski, D.C., Hurd, Y.L., Roussos, P., Brennand, K.J., Barry, G., 2018. THC exposure of human iPSC neurons impacts genes associated with neuropsychiatric disorders. Transl Psychiatry 8, 89.

Hartman, R.L., Brown, T.L., Milavetz, G., Spurgin, A., Gorelick, D.A., Gaffney, G., Huestis, M.A., 2016. Controlled vaporized cannabis, with and without alcohol: subjective effects and oral fluid-blood cannabinoid relationships. Drug Test Anal 8, 690-701.

Howlett, A.C., 2005. Cannabinoid receptor signaling. Handb Exp Pharmacol, 53-79.

Kathuria, A., Nowosiad, P., Jagasia, R., Aigner, S., Taylor, R.D., Andreae, L.C., Gatford, N.J.F., Lucchesi, W., Srivastava, D.P., Price, J., 2018. Stem cell-derived neurons from autistic individuals with SHANK3 mutation show morphogenetic abnormalities during early development. Mol Psychiatry 23, 735-746.

Kenakin, T., 2019. Biased Receptor Signaling in Drug Discovery. Pharmacol Rev 71, 267-315.

Kokona, D., Thermos, K., 2015. Synthetic and endogenous cannabinoids protect retinal neurons from AMPA excitotoxicity in vivo, via activation of CB1 receptors: Involvement of PI3K/Akt and MEK/ERK signaling pathways. Experimental Eye Research 136, 45-58.

Lu, H.C., Mackie, K., 2016. An Introduction to the Endogenous Cannabinoid System. Biol Psychiatry 79, 516-525.

Marsot, A., Audebert, C., Attolini, L., Lacarelle, B., Micallef, J., Blin, O., 2016. Comparison of Cannabinoid Concentrations in Plasma, Oral Fluid and Urine in Occasional Cannabis Smokers After Smoking Cannabis Cigarette. J Pharm Pharm Sci 19, 411-422.

Matsuda, L.A., Lolait, S.J., Brownstein, M.J., Young, A.C., Bonner, T.I., 1990. Structure of a cannabinoid receptor and functional expression of the cloned cDNA. Nature 346, 561-564.

Miller, L.K., Devi, L.A., 2011. The highs and lows of cannabinoid receptor expression in disease: mechanisms and their therapeutic implications. Pharmacol Rev 63, 461-470.

Moldzio, R., Pacher, T., Krewenka, C., Kranner, B., Novak, J., Duvigneau, J.C., Rausch, W.D., 2012. Effects of cannabinoids Delta(9)-tetrahydrocannabinol, Delta(9)-tetrahydrocannabinolic acid and cannabidiol in MPP+ affected murine mesencephalic cultures. Phytomedicine 19, 819-824.

Murray, R.M., Englund, A., Abi-Dargham, A., Lewis, D.A., Di Forti, M., Davies, C., Sherif, M., McGuire, P., D'Souza, D.C., 2017. Cannabis-associated psychosis: Neural substrate and clinical impact. Neuropharmacology 124, 89-104.

Namekata, K., Harada, C., Guo, X., Kimura, A., Kittaka, D., Watanabe, H., Harada, T., 2012. Dock3 Stimulates Axonal Outgrowth via GSK-3β-Mediated Microtubule Assembly. The Journal of Neuroscience 32, 264-274.

Njoo, C., Agarwal, N., Lutz, B., Kuner, R., 2015. The Cannabinoid Receptor CB1 Interacts with the WAVE1 Complex and Plays a Role in Actin Dynamics and Structural Plasticity in Neurons. PLoS Biol 13, e1002286.

Obiorah, I.V., Muhammad, H., Stafford, K., Flaherty, E.K., Brennand, K.J., 2017. THC Treatment Alters Glutamate Receptor Gene Expression in Human Stem Cell-Derived Neurons. Mol Neuropsychiatry 3, 73-84.

Ozaita, A., Puighermanal, E., Maldonado, R., 2007. Regulation of PI3K/Akt/GSK-3 pathway by cannabinoids in the brain. J Neurochem 102, 1105-1114.

Parr, C.J.C., Yamanaka, S., Saito, H., 2017. An update on stem cell biology and engineering for brain development. Molecular Psychiatry 22, 808.

Pasman, J.A., Verweij, K.J.H., Gerring, Z., Stringer, S., Sanchez-Roige, S., Treur, J.L., Abdellaoui, A., Nivard, M.G., Baselmans, B.M.L., Ong, J.S., Ip, H.F., van der Zee, M.D., Bartels, M., Day, F.R., Fontanillas, P., Elson, S.L., de Wit, H., Davis, L.K., MacKillop, J., Derringer, J.L., Branje, S.J.T., Hartman, C.A., Heath, A.C., van Lier, P.A.C., Madden, P.A.F., Magi, R., Meeus, W., Montgomery, G.W., Oldehinkel, A.J., Pausova, Z., Ramos-Quiroga, J.A., Paus, T., Ribases, M., Kaprio, J., Boks, M.P.M., Bell, J.T., Spector, T.D., Gelernter, J., Boomsma, D.I., Martin, N.G., MacGregor, S., Perry, J.R.B., Palmer, A.A., Posthuma, D., Munafo, M.R., Gillespie, N.A., Derks, E.M., Vink, J.M., 2018. GWAS of lifetime cannabis use reveals new risk loci, genetic overlap with psychiatric traits, and a causal influence of schizophrenia. Nat Neurosci.

Pertwee, R.G., Howlett, A.C., Abood, M.E., Alexander, S.P.H., Di Marzo, V., Elphick, M.R., Greasley, P.J., Hansen, H.S., Kunos, G., Mackie, K., Mechoulam, R., Ross,

R.A., 2010. International Union of Basic and Clinical Pharmacology. LXXIX. Cannabinoid Receptors and Their Ligands: Beyond CB₁ and CB₂. Pharmacological Reviews 62, 588-631.

Roland, A.B., Ricobaraza, A., Carrel, D., Jordan, B.M., Rico, F., Simon, A., Humbert-Claude, M., Ferrier, J., McFadden, M.H., Scheuring, S., Lenkei, Z., 2014. Cannabinoid-induced actomyosin contractility shapes neuronal morphology and growth. Elife 3, e03159.

Ronen, D., Benvenisty, N., 2014. Sex-dependent gene expression in human pluripotent stem cells. Cell Rep 8, 923-932.

Sanchez, M.G., Ruiz-Llorente, L., Sanchez, A.M., Diaz-Laviada, I., 2003. Activation of phosphoinositide 3-kinase/PKB pathway by CB(1) and CB(2) cannabinoid receptors expressed in prostate PC-3 cells. Involvement in Raf-1 stimulation and NGF induction. Cell Signal 15, 851-859.

Scheyer, A.F., Melis, M., Trezza, V., Manzoni, O.J.J., 2019. Consequences of Perinatal Cannabis Exposure. Trends Neurosci 42, 871-884.

Schlicker, E., Timm, J., Zentner, J., Gothert, M., 1997. Cannabinoid CB1 receptor-mediated inhibition of noradrenaline release in the human and guinea-pig hippocampus. Naunyn Schmiedebergs Arch Pharmacol 356, 583-589.

Selley, D.E., Stark, S., Sim, L.J., Childers, S.R., 1996. Cannabinoid receptor stimulation of guanosine-5'-O-(3-[35S]thio)triphosphate binding in rat brain membranes. Life Sci 59, 659-668.

Shi, Y., Kirwan, P., Smith, J., Robinson, H.P., Livesey, F.J., 2012. Human cerebral cortex development from pluripotent stem cells to functional excitatory synapses. Nat Neurosci 15, 477-486, S471.

Shum, C., Macedo, S.C., Warre-Cornish, K., Cocks, G., Price, J., Srivastava, D.P., 2015. Utilizing induced pluripotent stem cells (iPSCs) to understand the actions of estrogens in human neurons. Horm Behav 74, 228-242.

Stanslowsky, N., Jahn, K., Venneri, A., Naujock, M., Haase, A., Martin, U., Frieling, H., Wegner, F., 2017. Functional effects of cannabinoids during dopaminergic specification of human neural precursors derived from induced pluripotent stem cells. Addict Biol 22, 1329-1342.

Tabata, H., Nakajima, K., 2003. Multipolar migration: the third mode of radial neuronal migration in the developing cerebral cortex. J Neurosci 23, 9996-10001.

Takahashi, K., Tanabe, K., Ohnuki, M., Narita, M., Ichisaka, T., Tomoda, K., Yamanaka, S., 2007. Induction of pluripotent stem cells from adult human fibroblasts by defined factors. Cell 131, 861-872.

Takahashi, K., Yamanaka, S., 2006. Induction of Pluripotent Stem Cells from Mouse Embryonic and Adult Fibroblast Cultures by Defined Factors. Cell 126, 663-676.

Tortoriello, G., Morris, C.V., Alpar, A., Fuzik, J., Shirran, S.L., Calvigioni, D., Keimpema, E., Botting, C.H., Reinecke, K., Herdegen, T., Courtney, M., Hurd, Y.L., Harkany, T., 2014. Miswiring the brain: Delta9-tetrahydrocannabinol disrupts cortical development by inducing an SCG10/stathmin-2 degradation pathway. Embo j 33, 668-685.

Vitalis, T., Laine, J., Simon, A., Roland, A., Leterrier, C., Lenkei, Z., 2008. The type 1 cannabinoid receptor is highly expressed in embryonic cortical projection neurons and negatively regulates neurite growth in vitro. Eur J Neurosci 28, 1705-1718.

Wang, X., Wang, Z., Yao, Y., Li, J., Zhang, X., Li, C., Cheng, Y., Ding, G., Liu, L., Ding, Z., 2011. Essential role of ERK activation in neurite outgrowth induced by alpha-lipoic acid. Biochim Biophys Acta 1813, 827-838.

Watson, S., Chambers, D., Hobbs, C., Doherty, P., Graham, A., 2008. The endocannabinoid receptor, CB1, is required for normal axonal growth and fasciculation. Mol Cell Neurosci 38, 89-97.

Wu, C.S., Zhu, J., Wager-Miller, J., Wang, S., O'Leary, D., Monory, K., Lutz, B., Mackie, K., Lu, H.C., 2010. Requirement of cannabinoid CB(1) receptors in cortical pyramidal neurons for appropriate development of corticothalamic and thalamocortical projections. Eur J Neurosci 32, 693-706.

Zheng, J., Shen, W.H., Lu, T.J., Zhou, Y., Chen, Q., Wang, Z., Xiang, T., Zhu, Y.C., Zhang, C., Duan, S., Xiong, Z.Q., 2008. Clathrin-dependent endocytosis is required for TrkB-dependent Akt-mediated neuronal protection and dendritic growth. J Biol Chem 283, 13280-13288.

Zorina, Y., Iyengar, R., Bromberg, K.D., 2010. Cannabinoid 1 receptor and interleukin-6 receptor together induce integration of protein kinase and transcription factor signaling to trigger neurite outgrowth. J Biol Chem 285, 1358-1370.

Acknowledgements

The study was supported by grants from the Wellcome Trust ISSF Grant (No. 097819) and the King's Health Partners Research and Development Challenge Fund, a fund administered on behalf of King's Health Partners by Guy's and St Thomas' Charity awarded to DPS; the Brain and Behavior Foundation (formally National Alliance for Research on Schizophrenia and Depression (NARSAD); Grant No. 25957), awarded to DPS; the Innovative Medicines Initiative Joint Undertaking under grant agreement no. 115300, resources of which are composed of financial contribution from the European Union's Seventh Framework Programme (FP7/2007-2013) and EFPIA

companies' in kind contribution (JP and DPS). This work was also supported by funds the European Autism Interventions (EU-AIMS), and the Innovative Medicines Initiative Joint Undertaking under grant agreement no. 115300, resources of which are composed of financial contribution from the European Union's Seventh Framework Programme (FP7/2007-2013) and EFPIA companies' in kind contribution (JP, DPS and LCA); a Medical Research Council 4-year PhD studentship to SET, and funds from the Mortimer D Sackler Foundation and the Sackler Institute for Translational Neurodevelopment (RDT). SB has received support from the NIHR (NIHR Clinician Scientist Award; NIHR CS-11-001) and the UK MRC (MR/J012149/1). We thank the Wohl Cellular Imaging Centre (WCIC) at the IoPPN, Kings College, London, for help with microscopy.

Author contributions

C.S., L.D., E.A., K.W.C., S.E.T., R.D.T., L.C.A and D.P.S. carried out experiments and data analysis; N.J.B., J.P. and S.B. provided reagents, assistance in experimental design and editing of manuscript; C.S., L.D. and D.P.S. wrote the manuscript; D.P.S. designed the project.

Competing Interests

Authors declare no conflict of interest

Figure Legends

Figure 1: Generation of cortical neurons from hiPSCs. (A) Schematic of hiPSC differentiation protocol used. **(B)** Representative images of hiPSCs, NPCs and neurons immunostained for markers of specific cell linages. **(C)** Number of DAPI positive cells expressing markers of hiPSC, NPC and neuronal cell fate; error bars represent standard deviations (SD). **(D-G)** Expression profile of cell fate markers determined between day 7 and 50 following induction of neural differentiation; error bars represent SD.

Figure 2: Expression of cannabinoid receptors in hiPSC-neurons. (A) Expression of CB1R in NPCs and neurons in three independent hiPSC lines. In all three lines, CB1R expression increases as cells differentiate into neurons: ($F(2,12)=6.49$, $p < 0.05$, Bonferroni Post Hoc, ***, $p < 0.001$, two-way ANOVA; n = 3 independent cultures for each line). **(B)** Comparison of the expression of CB1R, CB2R, GPR55 and TRPV1 receptors in day 30 hiPSC-neurons. Whereas CB1R is highly expressed, no expression of CB2R, GPR55 or TRPV1 receptors was detected in three hiPSC-lines: ($F(6,12)=1.896$, $p < 0.05$, Bonferroni Post Hoc, ***, $p < 0.001$, two-way ANOVA; n = 2 independent cultures for each line). **(C)** Western blot demonstrating expression of CB1R in day 30 hiPSC-neurons derived from 2 independent hiPSC-lines. A prominent band is observed at ~53 kDa, predicted molecular weight of CB1R. **(D)** Representative confocal images of day 30 hiPSC-neurons immunostained for MAP2 (dendrites) and CB1R. Immunoreactive puncta for CB1R can be found along MAP2-positive neurites. Insets are of high magnification zooms of dendrite highlighted by white box in main image. Scale bar = 5 µm.

Figure 3: Negative regulation of neurite outgrowth in hiPSC-neurons by 2AG. (A) Representative images of MAP2 stained day 30 hiPSC-neurons as imaged using the Opera Phenix High Content Imager. **(B)** Assessing of the number of DAPI-positive MAP2 neurons demonstrates no difference on overall neuronal number across conditions. Data are presented for each individual hiPSC-line: data was generated from 3 independent cultures for each independent hiPSC line. **(C, D)** Assessment of average neurite number **(C)** and average branch number **(D)** revealed no difference between conditions. **(E)** Treatment with 2AG for 24 hours significantly reduced total neurite length compared to vehicle control. Scale bar = 50 µm.

Figure 4: Δ^9-THC negatively influences neurite outgrowth in hiPSC-neurons. (A) Representative images of MAP2 stained day 30 hiPSC-neurons following 24 hour treatment with vehicle or Δ^9-THC, as imaged using the Opera Phenix High Content Imager. **(B)** Assessing of the number of DAPI-positive MAP2 neurons demonstrates no difference on overall neuronal number across conditions. Data are presented for each individual hiPSC-line: data was generated from 3 independent cultures for each independent hiPSC line. **(C, D)** Assessment of average neurite number **(C)** and average branch number **(D)** revealed no difference between conditions. **(E)** Treatment with Δ^9-THC for 24 hours significantly reduced total neurite length compared to vehicle control. Scale bar = 50 µm.

Figure 5: 2AG decreases ERK1/2 phosphorylation and Δ^9-THC negative regulate ERK1/2 and Akt phosphorylation. (A) Western blot analysis of day 30 hiPSC-neurons treated with 2AG for 15 or 30 minutes compared to vehicle control conditions.

Western blots probed for total and pERK1/2, revealed a significant decrease in active (phosphorylated) ERK1/2 levels after 30 minutes of 2AG treatment ($F(2,6)=6.593$, $p < 0.05$, Tukey Post Hoc, *, $p < 0.05$, one-way ANOVA; n = 3 per condition from 3 independent hiPSC-lines). **(B, C)** Western blot analysis of day 30 hiPSC-neurons treated with 2AG for 15 or 30 minutes compared to vehicle control conditions. Western blots probed for total and active (phosphorylated) Akt and GSK3β; no difference was observed between conditions. **(D)** Western blot analysis of day 30 hiPSC-neurons treated with Δ^9-THC for 15 or 30 minutes compared to vehicle control conditions. Western blots probed for total and pERK1/2, revealed a significant decrease in active (phosphorylated) ERK1/2 levels after 30 minutes of Δ^9-THC treatment ($F(2,6)=8.299$, $p < 0.05$, Tukey Post Hoc, *, $p < 0.05$, one-way ANOVA; n = 3 per condition from 3 independent hiPSC-lines). **(E)** Assessment of pAkt levels also revealed a reduction in active levels of Akt following treatment with Δ^9-THC ($F(2,6)=9.557$, $p < 0.05$, Tukey Post Hoc, *, $p < 0.05$, one-way ANOVA; n = 3 per condition from 3 independent hiPSC-lines). **(F)** Cell lysates were also assessed for levels of active (phosphorylated) GSK3β; no difference was observed between conditions. Full blots are shown in **Supplementary Figure 5 & 6**.

Figure 6: CB1R antagonist SR 141716A blocks negative regulation of ERK1/2 and Akt phosphorylation by 2AG and Δ^9-THC. (A) Western blot analysis of day 30 hiPSC-neurons treated with vehicle, 2AG or Δ^9-THC (30 minutes) with or without pre-treatment with inverse antagonist SR 141716A (20 nM). Western blots probed for total and pERK1/2, revealed that SR 141716A blocked 2AG or Δ^9-THC induced decrease in active (phosphorylated) ERK1/2 levels after 30 minutes. **(B)** Cell lysates were also

assessed for levels of pAkt. This revealed that SR 141716A blocked Δ^9-THC decrease in pAkt levels. Full blots are shown in **Supplementary Figure 7**.

Figure 7: Negative regulation of neurite outgrowth by 2AG and Δ^9-THC is attenuated by SR 141716A. (A) Representative images of MAP2 stained day 30 hiPSC-neurons following 24 hour treatment with vehicle, 2AG or Δ^9-THC, with or without co-treatment with inverse antagonist SR 141716A (20 nM). **(B)** Assessing of total neurite length in all conditions. Data are presented for each individual hiPSC-line: data was generated from 3 independent cultures for each independent hiPSC line. Treatment with 2AG or Δ^9-THC for 24 hours significantly reduced total neurite length compared to vehicle control. This effect was attenuated by SR 141716A. Scale bar = 50 µm.

Table 1. List of antibodies used for immunohistochemistry

Antibody	Type	Host	Dilution	Supplier	Catalog Number
NESTIN	Monoclonal	Mouse	1:500	R&D Systems	MAB1259
OCT4	Monoclonal	Mouse	1:200	Santa cruz	Sc5279
PAX6	Polyclonal	Rabbit	1:200	Proteintech grPooup	12323-1-AP
SOX11	Polyclonal	Rabbit	1:50	Santa cruz	Sc20096
NANOG	Polyclonal	Goat	5ug/ml	R&D Systems	AF1997
ZNF521	Polyclonal	Rabbit	1:100	Atlas Antibodies	HPA023056
FOXG1	Polyclonal	Rabbit	1:500	Abcam	Ab18259
TBR1	Polyclonal	Rabbit	1:500	Abcam	Ab31940
TBR2	Polyclonal	Rabbit	1ug/ml	Abcam	Ab23345
BRN2	Polyclonal	Rabbit	1:500	Santa cruz	Sc28594
MAP2	Polyclonal	Chicken	1:1000	Abcam	Ab92434
CB1R	Polyclonal	Rabbit	1:50	Abcam	ab23703
Erk 1/2	Monoclonal	Mouse	1:2000	Cell signaling	L34F12
p-Erk	Polyclonal	Rabbit	1:1000	Cell signaling	T202 Y204
GSK3-beta	Monoclonal	Mouse	1:1000	Cell signaling	3D10
p- GSK3-beta	Polyclonal	Rabbit	1:1000	Cell signaling	D85E12
Akt	Monoclonal	Mouse	1:2000	Cell signaling	40D4
p-Akt	Polyclonal	Rabbit	1:1000	Cell signaling	5473


A
hiPSCs
Neuralization
Neurons
D0
Dual SMAD inhibition
D8
D20
+ DAPT
(Banked NPCs)
D30

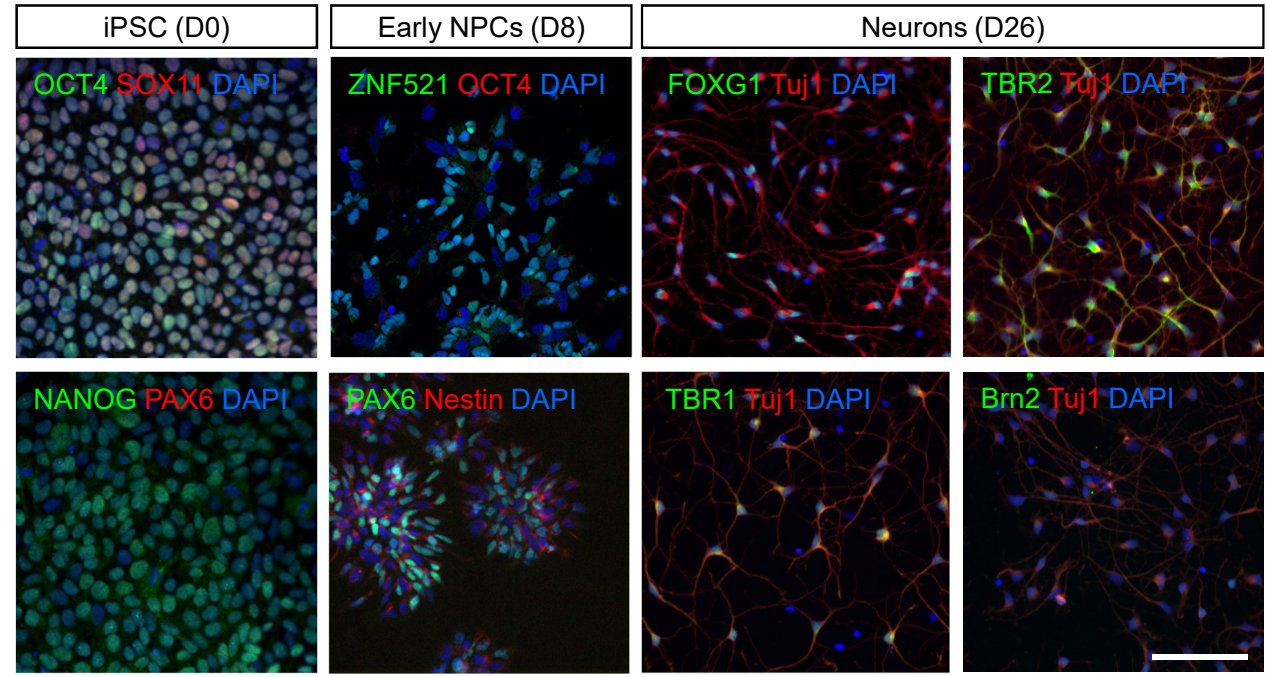
B
iPSC (D0)
Early NPCs (D8)
Neurons (D26)
OCT4 SOX11 DAPI
ZNF521 OCT4 DAPI
FOXG1 Tuj1 DAPI
TBR2 Tuj1 DAPI
NANOG PAX6 DAPI
PAX6 Nestin DAPI
TBR1 Tuj1 DAPI
Brn2 Tuj1 DAPI

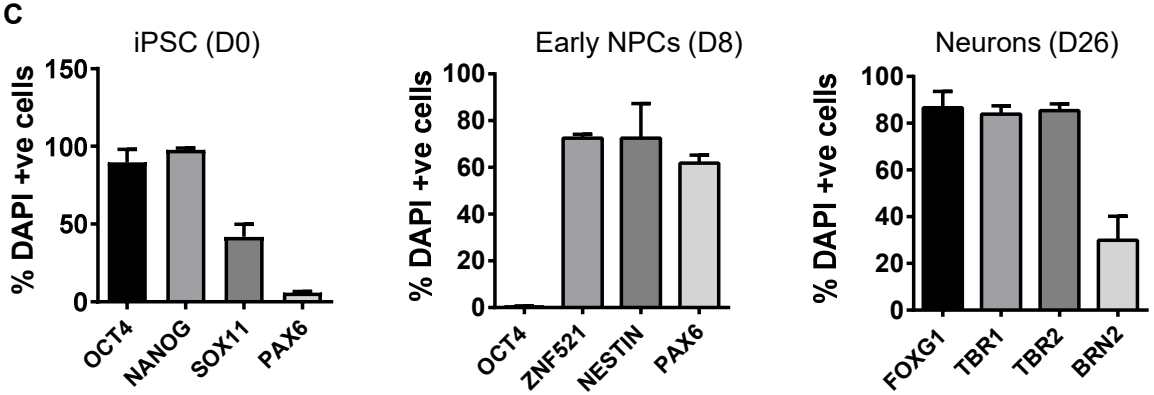
C
iPSC (D0)
% DAPI +ve cells
OCT4
NANOG
SOX11
PAX6
Early NPCs (D8)
% DAPI +ve cells
OCT4
ZNF521
NESTIN
PAX6
Neurons (D26)
% DAPI +ve cells
FOXG1
TBR1
TBR2
BRN2

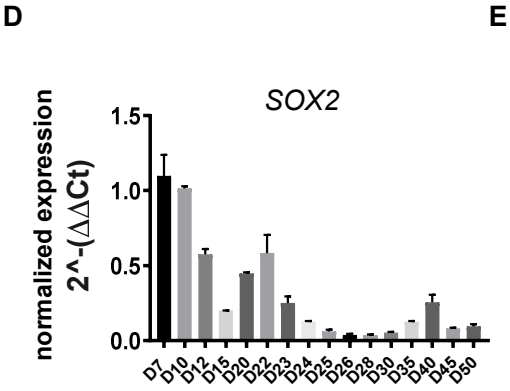
D
SOX2
normalized expression
2^-(ΔΔCt)

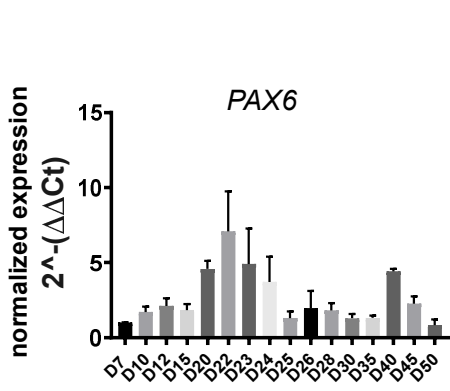
E
PAX6
normalized expression
2^-(ΔΔCt)

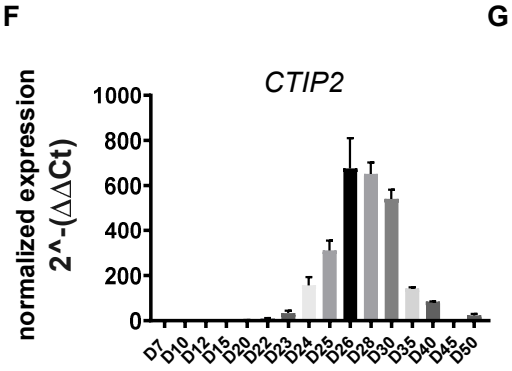
F
CTIP2
normalized expression
2^-(ΔΔCt)

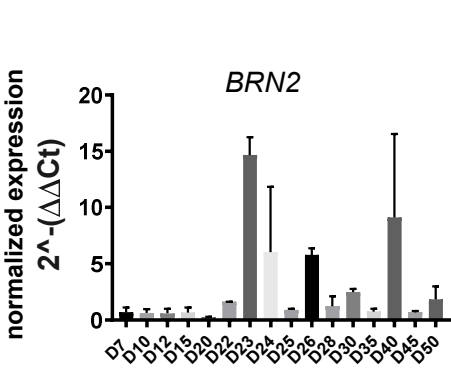
G
BRN2
normalized expression
2^-(ΔΔCt)

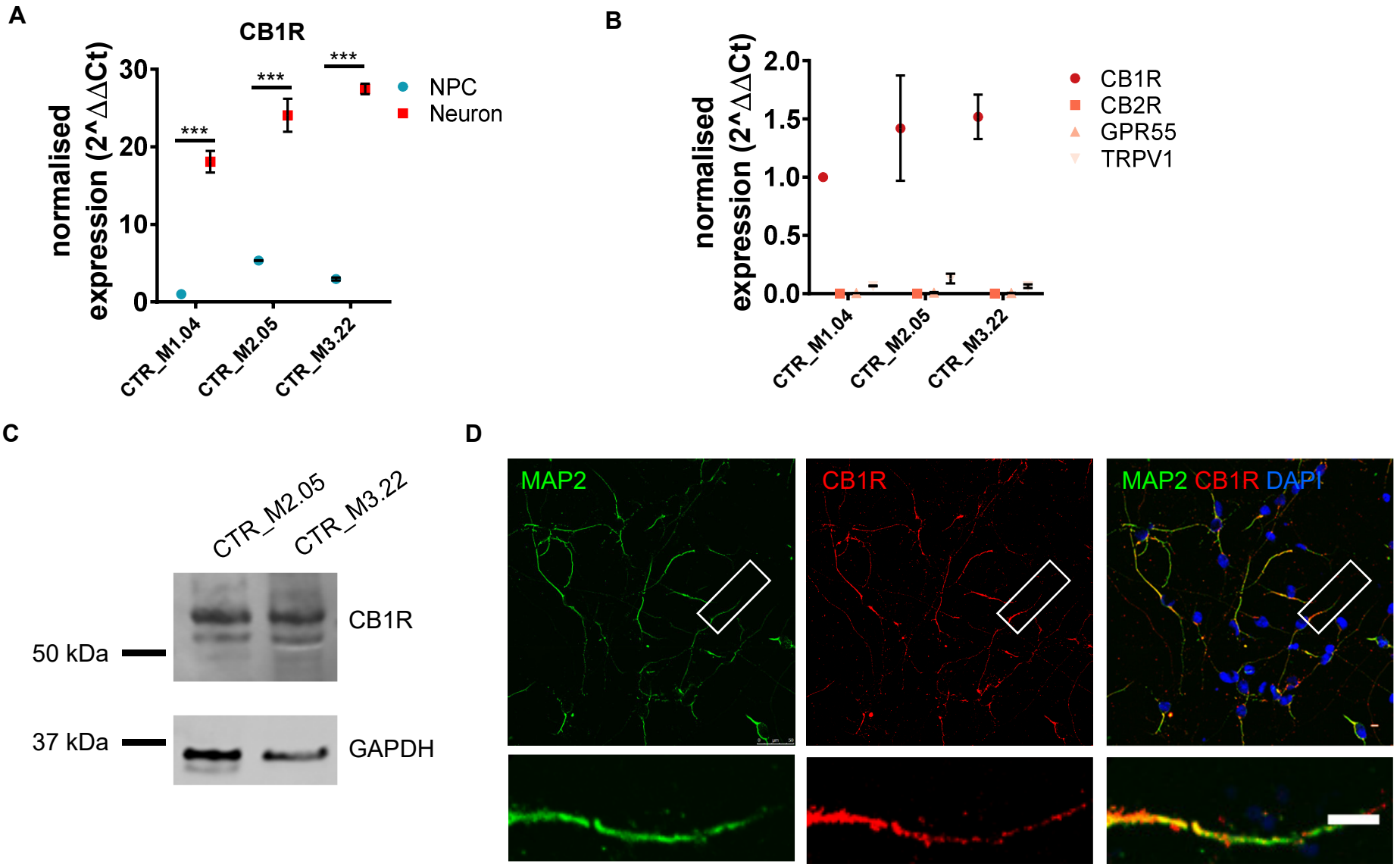
A
CB1R
normalised expression (2^ΔΔCt)
30
20
10
0
***
***
***
NPC
Neuron
CTR_M1.04
CTR_M2.05
CTR_M3.22
B
normalised expression (2^ΔΔCt)
2.0
1.5
1.0
0.5
0.0
CB1R
CB2R
GPR55
TRPV1
CTR_M1.04
CTR_M2.05
CTR_M3.22
C
CTR_M2.05
CTR_M3.22
50 kDa
CB1R
37 kDa
GAPDH
D
MAP2
CB1R
MAP2 CB1R DAPI

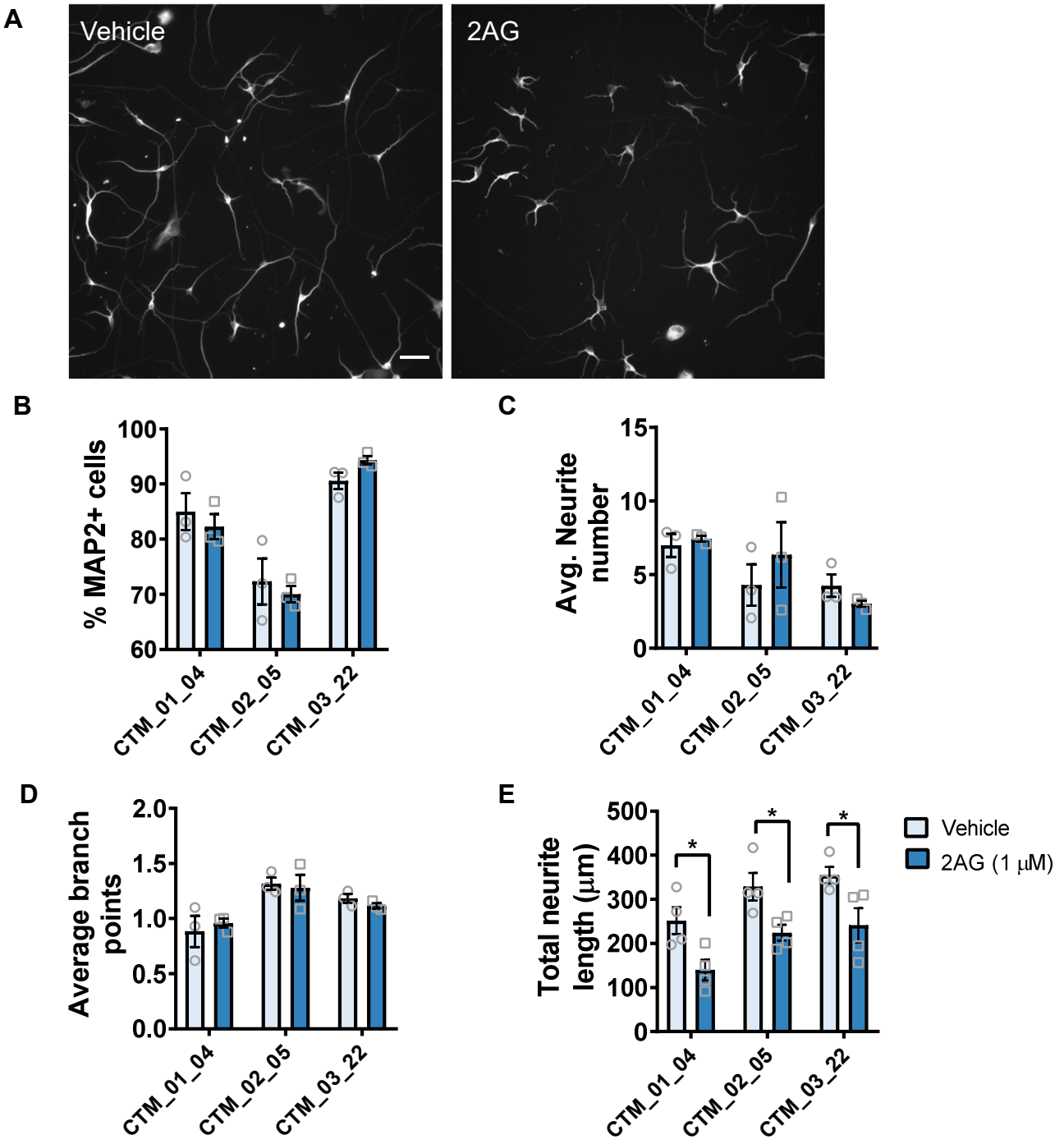
A
Vehicle
2AG
B
% MAP2+ cells
100
90
80
70
60
CTM_01_04
CTM_02_05
CTM_03_22
C
Avg. Neurite number
15
10
5
0
CTM_01_04
CTM_02_05
CTM_03_22
D
Average branch points
2.0
1.5
1.0
0.5
0.0
CTM_01_04
CTM_02_05
CTM_03_22
E
Total neurite length (μm)
500
400
300
200
100
0
*
*
*
CTM_01_04
CTM_02_05
CTM_03_22
Vehicle
2AG (1 μM)

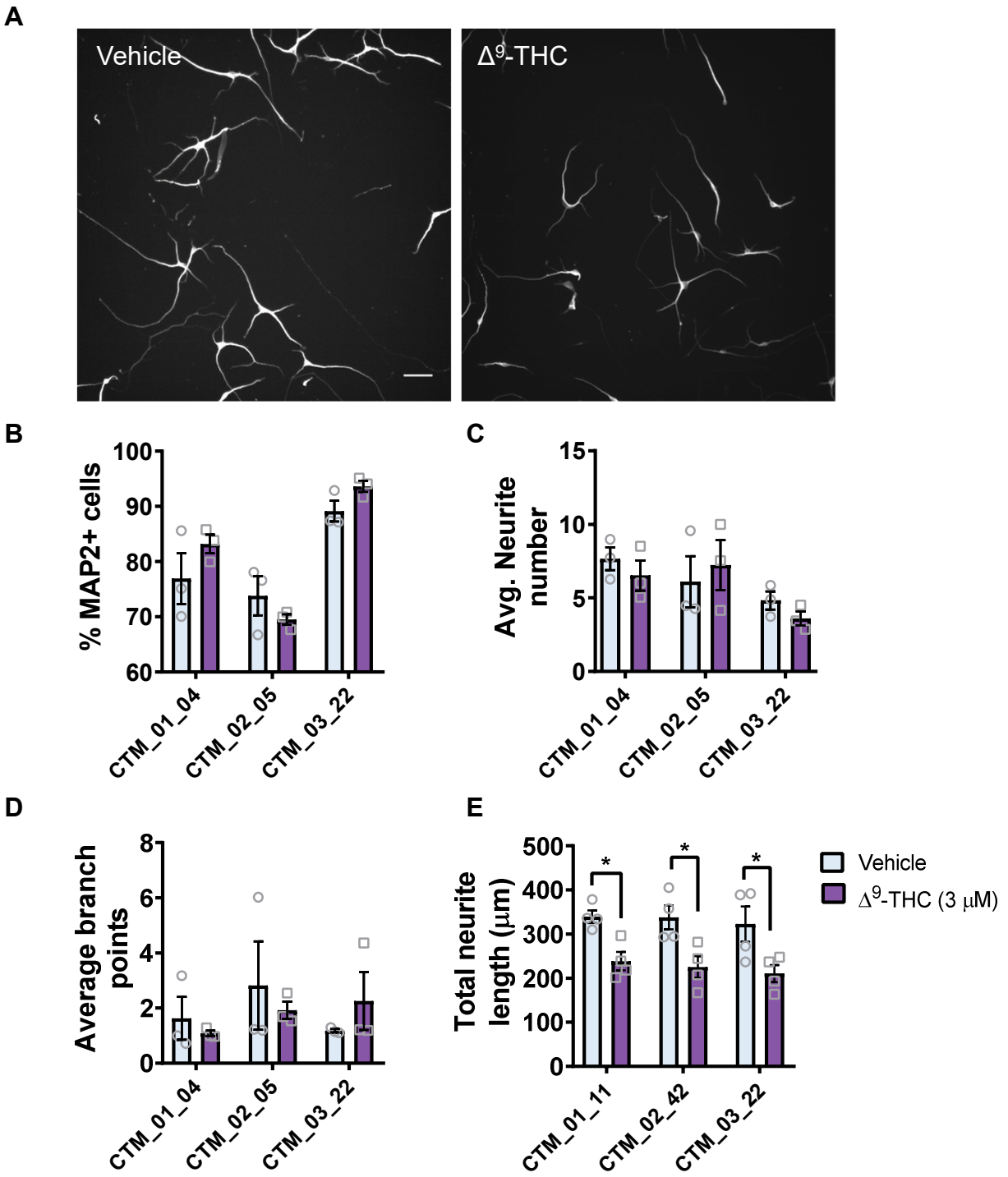
A
Vehicle
Δ9-THC
B
% MAP2+ cells
100
90
80
70
60
CTM_01_04
CTM_02_05
CTM_03_22
C
Avg. Neurite number
15
10
5
0
CTM_01_04
CTM_02_05
CTM_03_22
D
Average branch points
8
6
4
2
0
CTM_01_04
CTM_02_05
CTM_03_22
E
Total neurite length (μm)
500
400
300
200
100
0
*
*
*
CTM_01_11
CTM_02_42
CTM_03_22
Vehicle
Δ9-THC (3 μM)

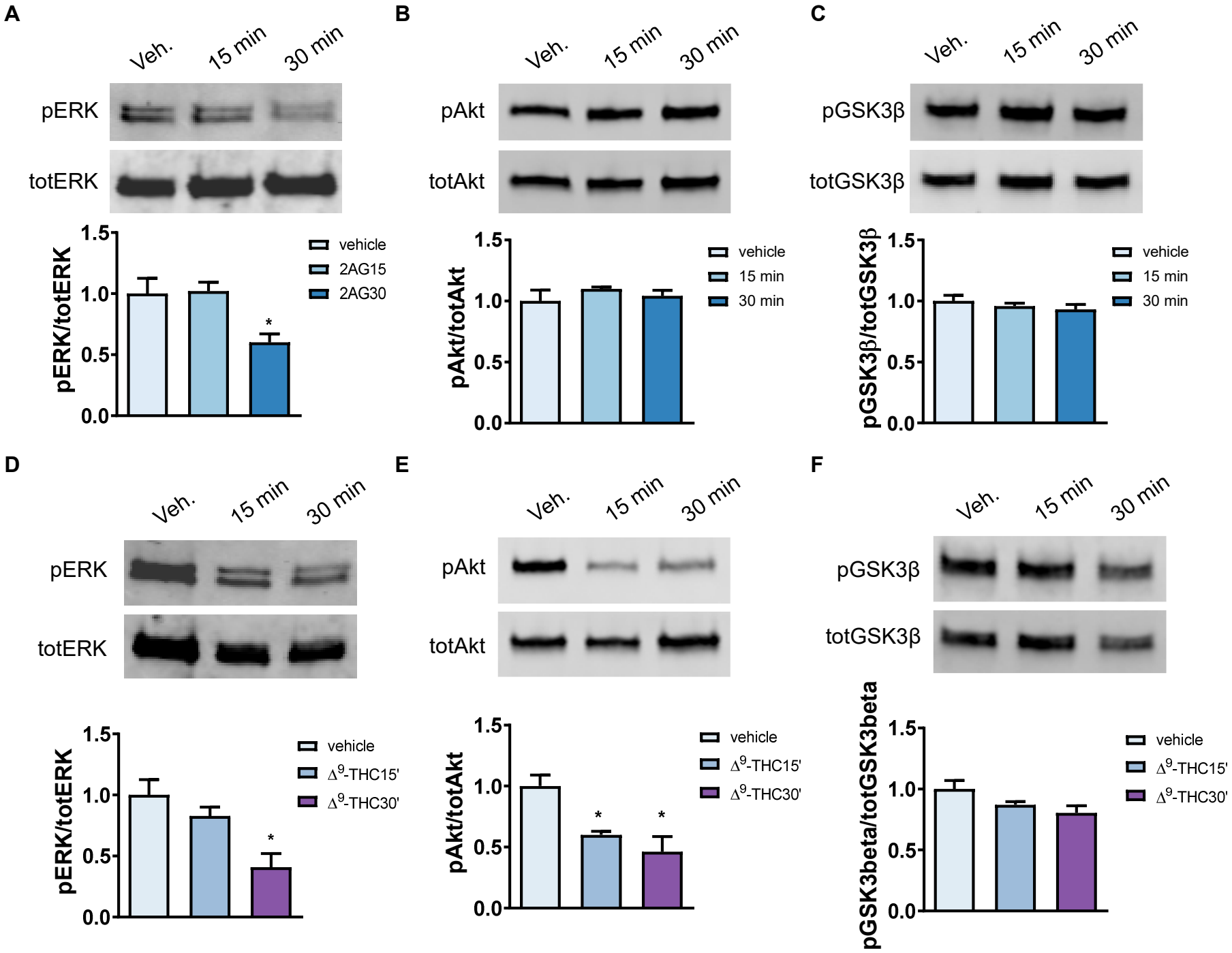
A
Veh.
15 min
30 min
pERK
totERK
pERK/totERK
1.5
1.0
0.5
0.0
*
vehicle
2AG15
2AG30
B
Veh.
15 min
30 min
pAkt
totAkt
pAkt/totAkt
1.5
1.0
0.5
0.0
vehicle
15 min
30 min
C
Veh.
15 min
30 min
pGSK3β
totGSK3β
pGSK3β/totGSK3β
1.5
1.0
0.5
0.0
vehicle
15 min
30 min
D
Veh.
15 min
30 min
pERK
totERK
pERK/totERK
1.5
1.0
0.5
0.0
*
vehicle
Δ9-THC15'
Δ9-THC30'
E
Veh.
15 min
30 min
pAkt
totAkt
pAkt/totAkt
1.5
1.0
0.5
0.0
*
*
vehicle
Δ9-THC15'
Δ9-THC30'
F
Veh.
15 min
30 min
pGSK3β
totGSK3β
pGSK3beta/totGSK3beta
1.5
1.0
0.5
0.0
vehicle
Δ9-THC15'
Δ9-THC30'

A

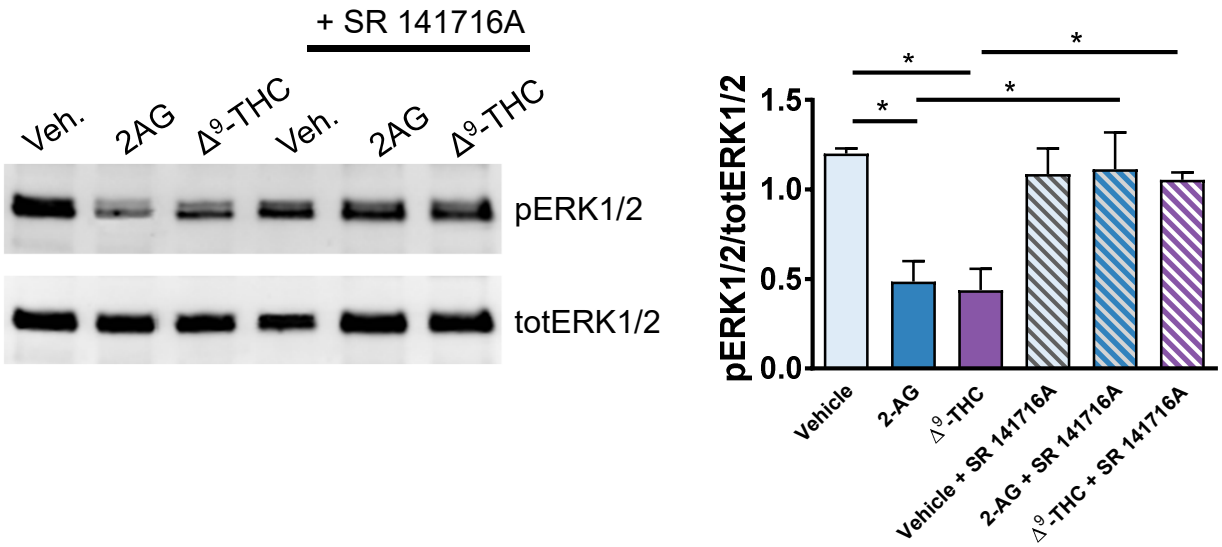
+ SR 141716A
Veh.
2AG
Δ9-THC
Veh.
2AG
Δ9-THC
pERK1/2
totERK1/2
pERK1/2/totERK1/2
1.5
1.0
0.5
0.0
*
*
*
*
Vehicle
2-AG
Δ9-THC
Vehicle + SR 141716A
2-AG + SR 141716A
Δ9-THC + SR 141716A

B

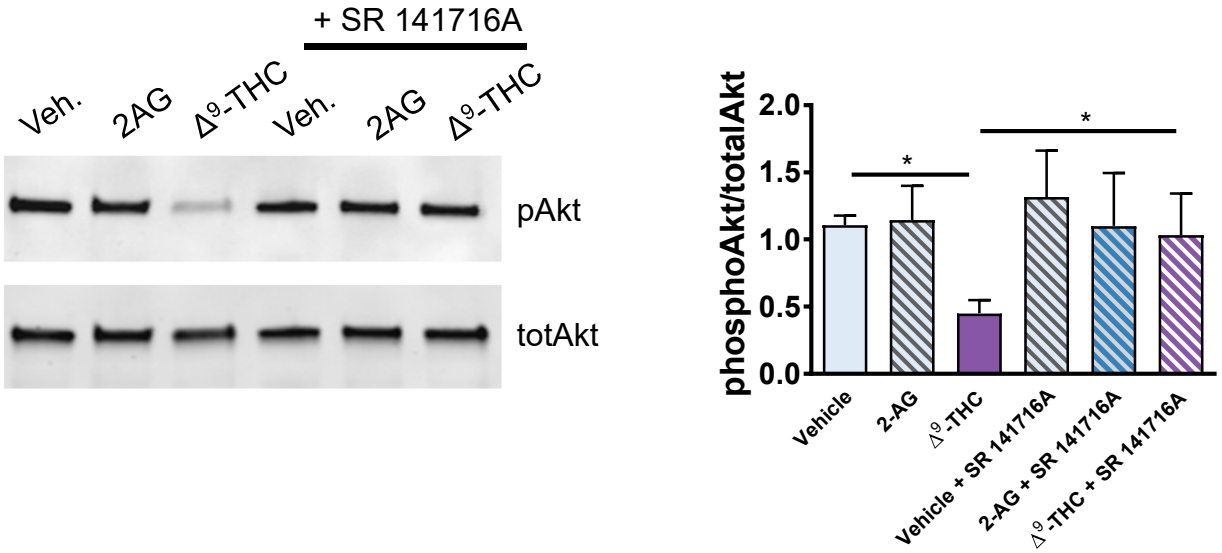
+ SR 141716A
Veh.
2AG
Δ9-THC
Veh.
2AG
Δ9-THC
pAkt
totAkt
phosphoAkt/totalAkt
2.0
1.5
1.0
0.5
0.0
*
*
Vehicle
2-AG
Δ9-THC
Vehicle + SR 141716A
2-AG + SR 141716A
Δ9-THC + SR 141716A

A

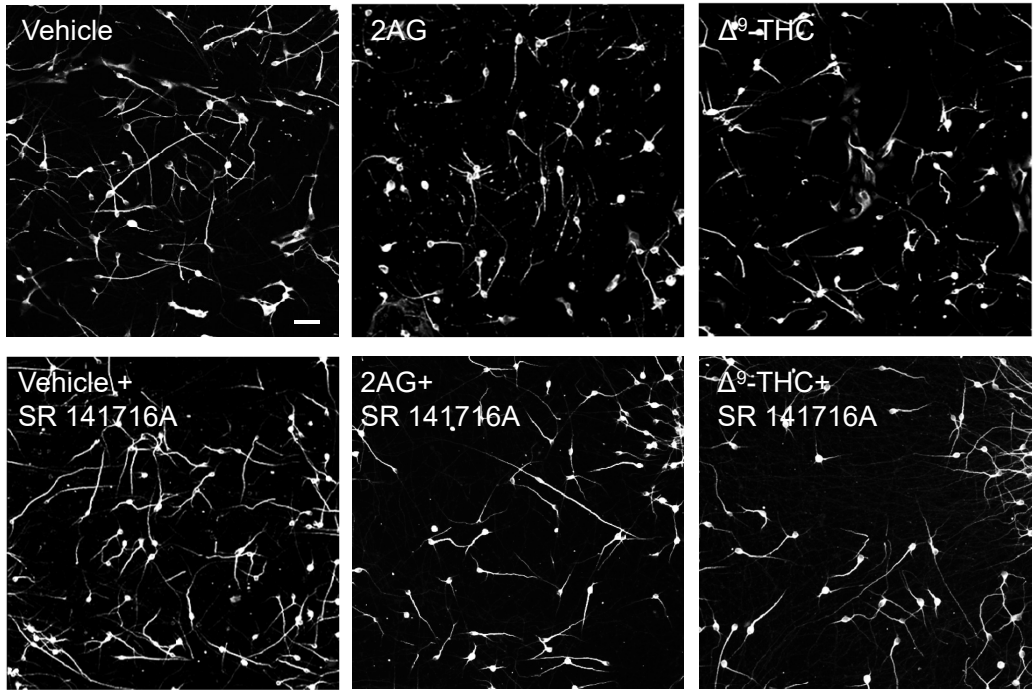
Vehicle
2AG
Δ9-THC
Vehicle +
SR 141716A
2AG+
SR 141716A
Δ9-THC+
SR 141716A

B

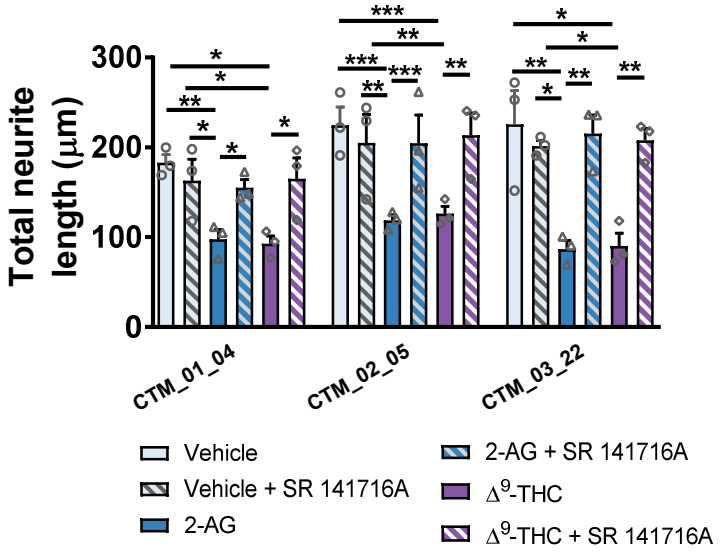
Total neurite length (µm)
300
200
100
0
CTM_01_04
CTM_02_05
CTM_03_22
Vehicle
Vehicle + SR 141716A
2-AG
2-AG + SR 141716A
Δ9-THC
Δ9-THC + SR 141716A

Δ^9-tetrahydrocannabinol and 2-AG decreases neurite outgrowth and differentially affects ERK1/2 and Akt signaling in hiPSC-derived cortical neurons.

Carole Shum[1,2], Lucia Dutan[1,2], Emily Annuario[1,2], Katherine Warre-Cornish[1,2], Samuel E. Taylor[2,3], Ruth D. Taylor[2,3], Laura C. Andreae[2,3], Noel J. Buckley[4], Jack Price[1,2,4], Sagnik Bhattacharyya[6]*, Deepak P. Srivastava[1,2]*

[1]Department of Basic and Clinical Neuroscience, The Maurice Wohl Clinical Neuroscience Institute, Institute of Psychiatry Psychology and Neuroscience, King's College London, London, SE5 8AF, UK; [2]MRC Centre for Neurodevelopmental Disorders, King's College London, London, UK; [3]Centre for Developmental Neurobiology, King's College London, London, UK, [4]Department of Psychiatry, University of Oxford, UK; [5]National Institute for Biological Standards and Control, South Mimms, UK [6]Department of Psychosis Studies, King's College London, London, SE5 8AF, UK.

* = corresponding authors: sagnik.2.bhattacharyya@kcl.ac.uk; deepak.srivastava@kcl.ac.uk

Supplementary Information:

Supplementary Methods

Supplementary Figures 1-8

Human induced pluripotent stem cells (hiPSCs)

hiPSC lines were generated from primary keratinocytes. Briefly, 1 x 10^5 primary hair root keratinocytes were reprogramed by introducing OCT4, SOX2, KLF4 and C-MYC factors with a CytoTune-iPS 2.0 Sendai expressing Reprogramming Kit (ThermoFisher, A16517). Transformed keratinocytes were plated onto an irradiated MEF feeder layer (Millipore) supplemented Epilife medium for ten days before switching to 'hES media', which consisted of KO-DMEM/F12 supplemented with 20% Knock-out serum replacement, Non-essential amino acids, Glutamax, β-mercaptoethanol (all from Life Technologies) and bFGF (10 ng/ml; Peprotech). After a further two weeks, reprogrammed colonies were selected and plated on Geltrex (Life technologies) coated Nunc treated multidishes (Thermo Scientific) into E8 media (Life Technologies). hiPSCs reprograming was validated by genome-wide expression profiling using Illumina Beadchip v4 and the bioinformatics tool 'Pluritest'. Additionally, the tri-lineage differentiation potential was stablished by embryoid body formation; ICCs to validate the expression of different pluripotency markers including Nanog, OCT4, SSEA4 and TRA1-81 and the alkaline phosphatase activity by Alkaline phosphatase expression kit (Milipore). The genomic stability was determined by G-banded karyotyping. hiPSCs were incubated in hypoxic conditions at 37°C and maintained in E8 media replaced every 24 hours until the cells monolayer reach ~95% confluence.

Electrophysiology

Electrophysiological recordings were obtained from hiPSC derived neurons differentiated for 64 days *in vitro*. Patch pipettes (4.0–7.5 MΩ) were pulled from borosilicate glass capillary tubes using a P97 Flaming/Brown Micropipette Puller

(Sutter Instruments). The internal patch solution contained (in mM) 135 K-Gluconate, 10 KCl, 1 MgCl2, 10 HEPES, 2 Na2 -ATP and 0.4 Na3 -GTP. All recordings were conducted at room temperature in neurobasal medium (0.1% BDNF, 0.01% Ascorbic acid, 2% B27, 1% Glutamax). Spontaneous currents were measured by whole cell voltage clamp recordings at a holding potential of −70mV. Current-voltage recordings were conducted from a holding potential of -70mV with increasing voltage steps of 2mV increments up to +20mV. Action potentials were recorded in current clamp from a holding potential of -6 mV, with 2pA current injection increments each of 500ms. Data were generated and acquired using an EPC10 amplifier (Heka Instruments, Bellmore, NY, USA) and the software PatchMaster.

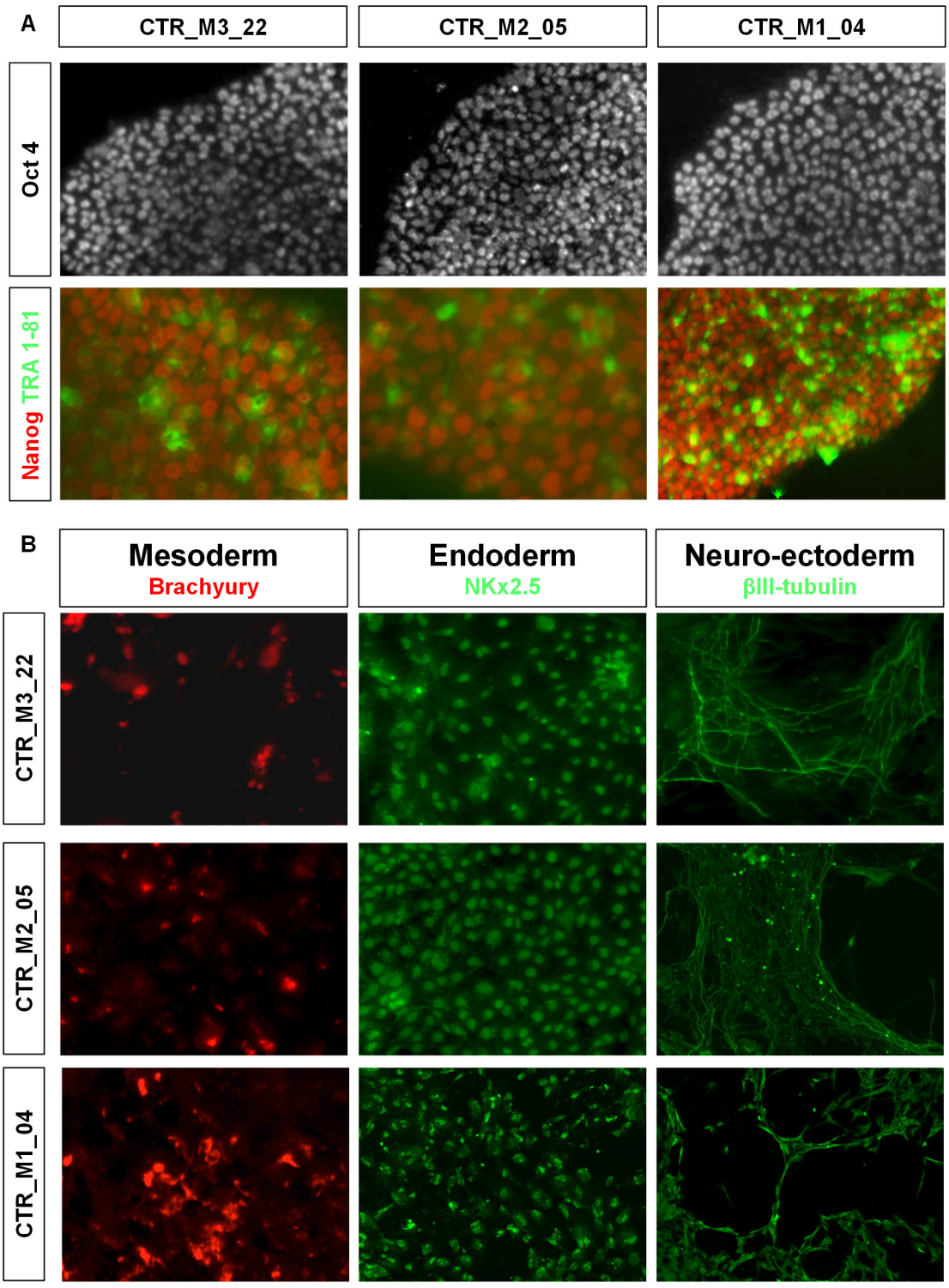

Supplementary Figure 1. Validation of hiPSC lines. **(A)** HiPSCs were immunostained for pluripotency markers Oct4, Nanog and Tra-18-1. **(B)** HiPSCs were further tested for their ability to generate cells from the 3 germ layers using an embyobody methodology (Cocks et al., 2014). All three hiPSC line demonstrated the ability to spontaneously generate mesoderm, endoderm and (neuro-)ectoderm cells.

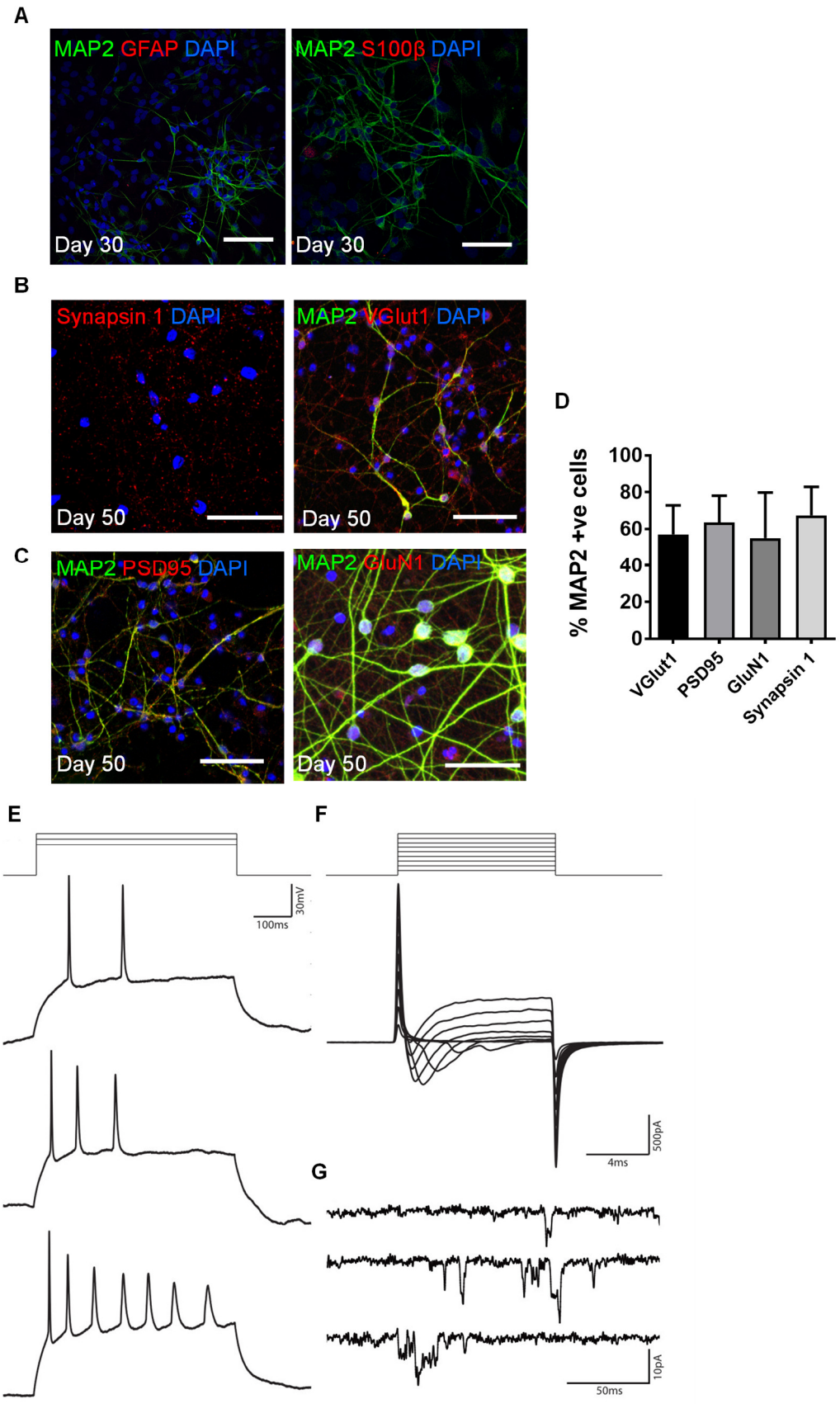

Supplementary Figure 2. Characterization of hiPSC-neurons. (A) Representative images of day 30 hiPSC-neurons immunostained for glia markers GFAP and S100β.

(B & C) Representative images of day 50 hiPSC-neuron immunostained for glutamatergic markers. **(D)** Number of MAP2 positive cells expressing VGlut1, PSD95, GluN1 and synapsin 1; error bars represent standard deviations (SD). **(E-F)** Whole cell patch clamp recordings obtained from day 64 hiPSC derived neurons. **(E)** Action potentials recorded in response to increasing current injection (24pA, 28pA and 32pA) in current clamp. **(F)** Voltage clamp recordings of the voltage activated currents elicited in response to 10ms long voltage steps from a holding potential of -70mV. Representative I-V traces at 10mV voltage increments. **(G)** Representative spontaneous current events recorded in voltage clamp at -70mV.

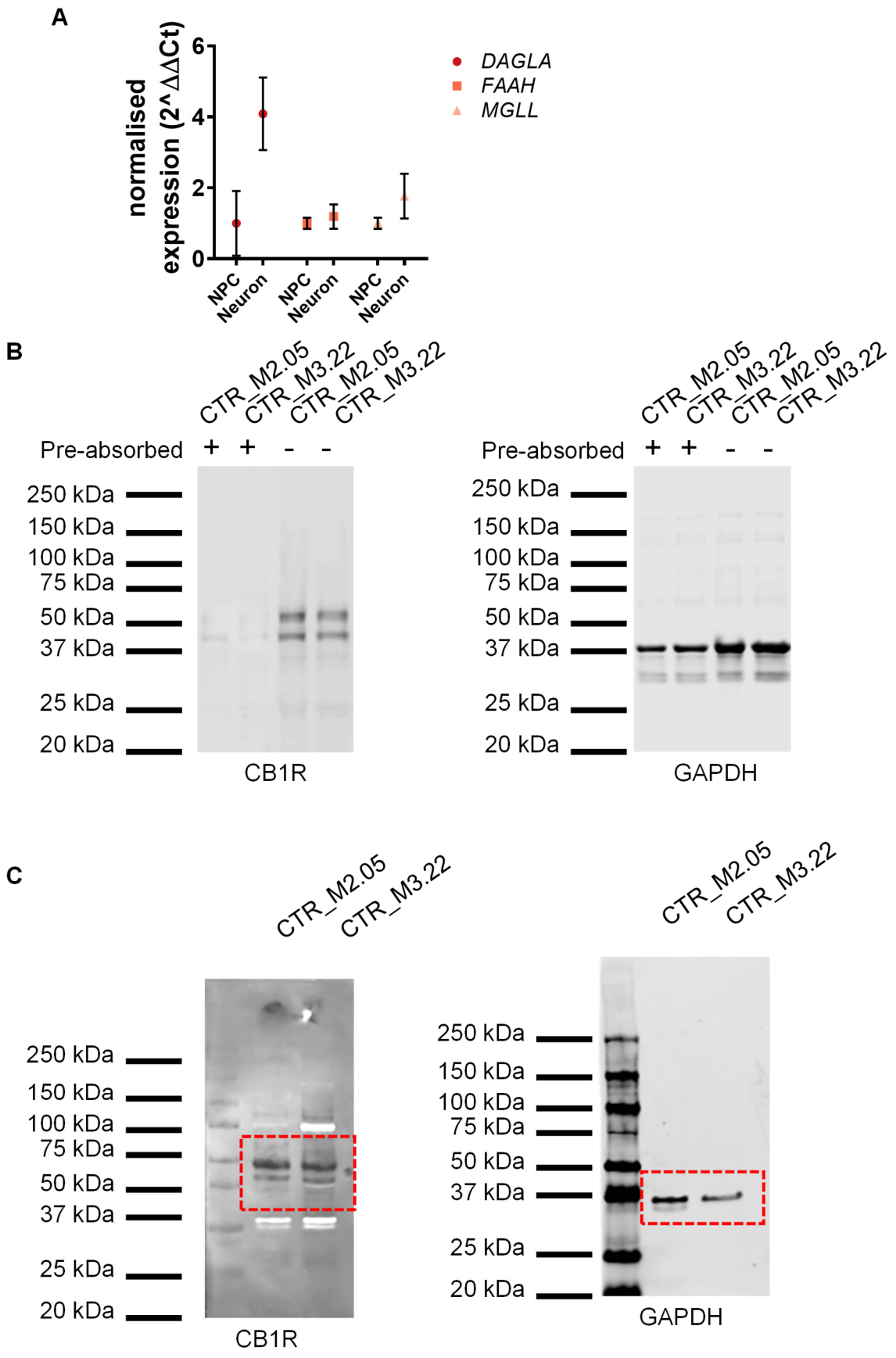

Supplementary Figure 3. Characterization of endocannaboid system in hiPSC-

neurons. (A) Expression of *DAGLA*, *FAAH* and *MGLL* CB1R in NPCs and neurons in three independent hiPSC lines. *DAGLA* expression increased as cells differentiate into neurons, whereas *FAAH* and *MGLL* expression did not altered between these two time points (two-way ANOVA; n = 3 independent cultures for each line).**(B)** Pre-absorption of CB1R antibody with antigenic peptide abolishes bands around 53kDa, predicted molecular weight of CB1R protein. **(C)**: Full length blot of western blot shown in main Figure 2C.

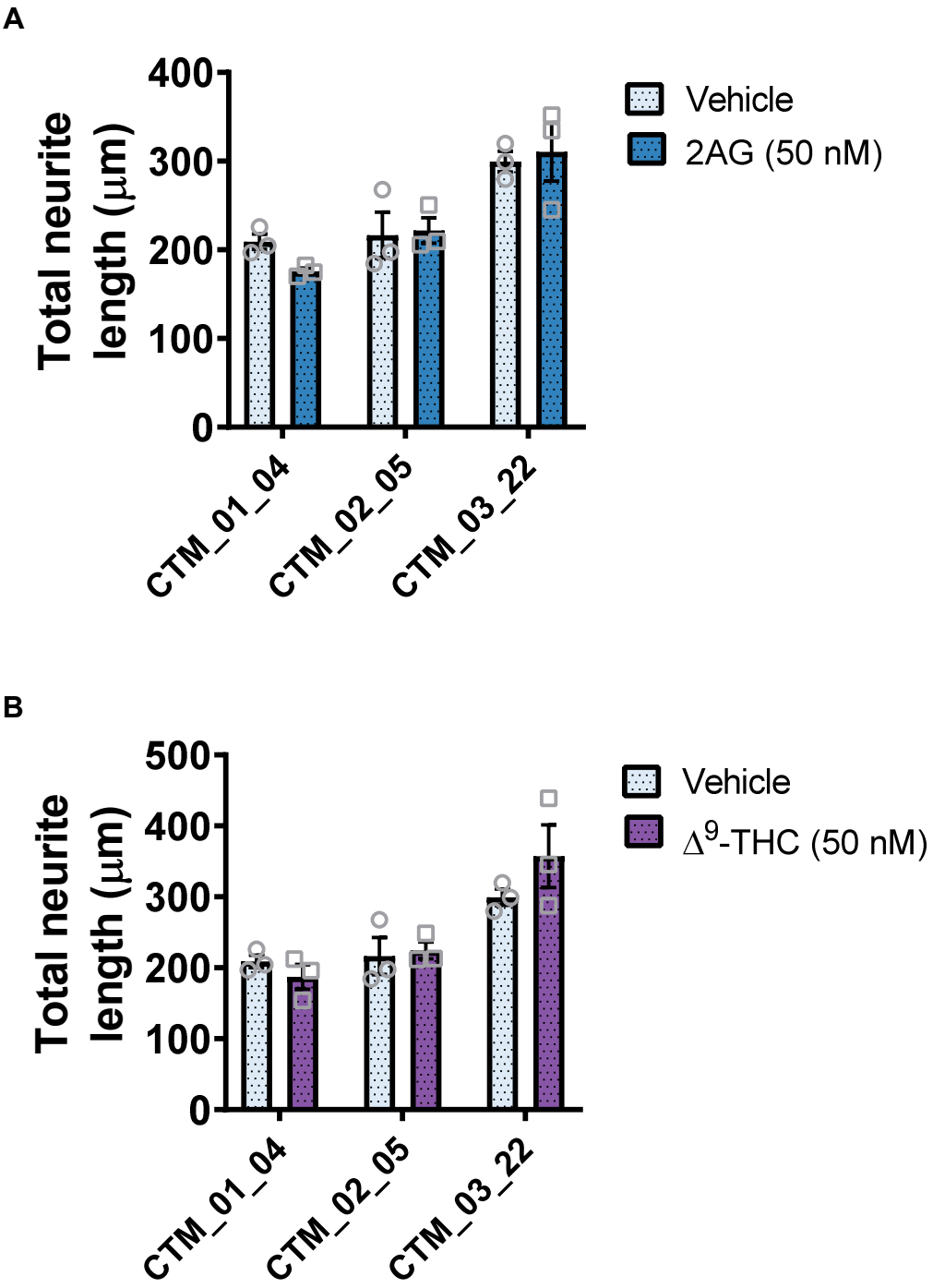

Supplementary Figure 4. Effect of low concentrations of 2AG and Δ^9-THC on neurite outgrowth in hiPSC-neurons. (A) Assessing total neurite length revealed that 50 nM 2AG (24 hours) had no effect on neurite outgrowth compared to vehicle control. **(B)** Assessment of total neurite length demonstrated that treatment with 50 nM Δ^9-THC for 24 hours had no effect on neurite length.

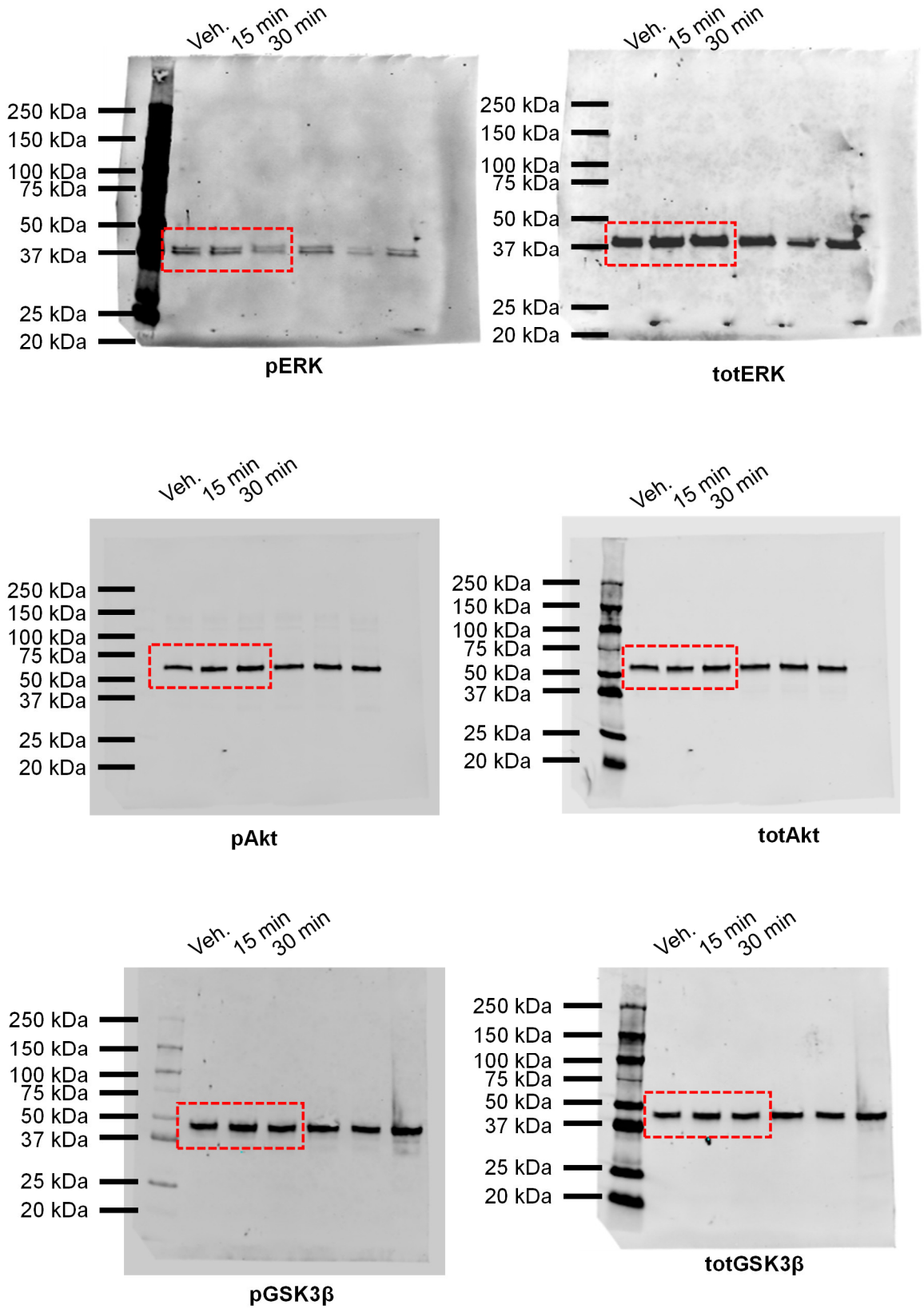

Supplementary Figure 5. Full length blot of western blot shown in main Figure 5 A to C.

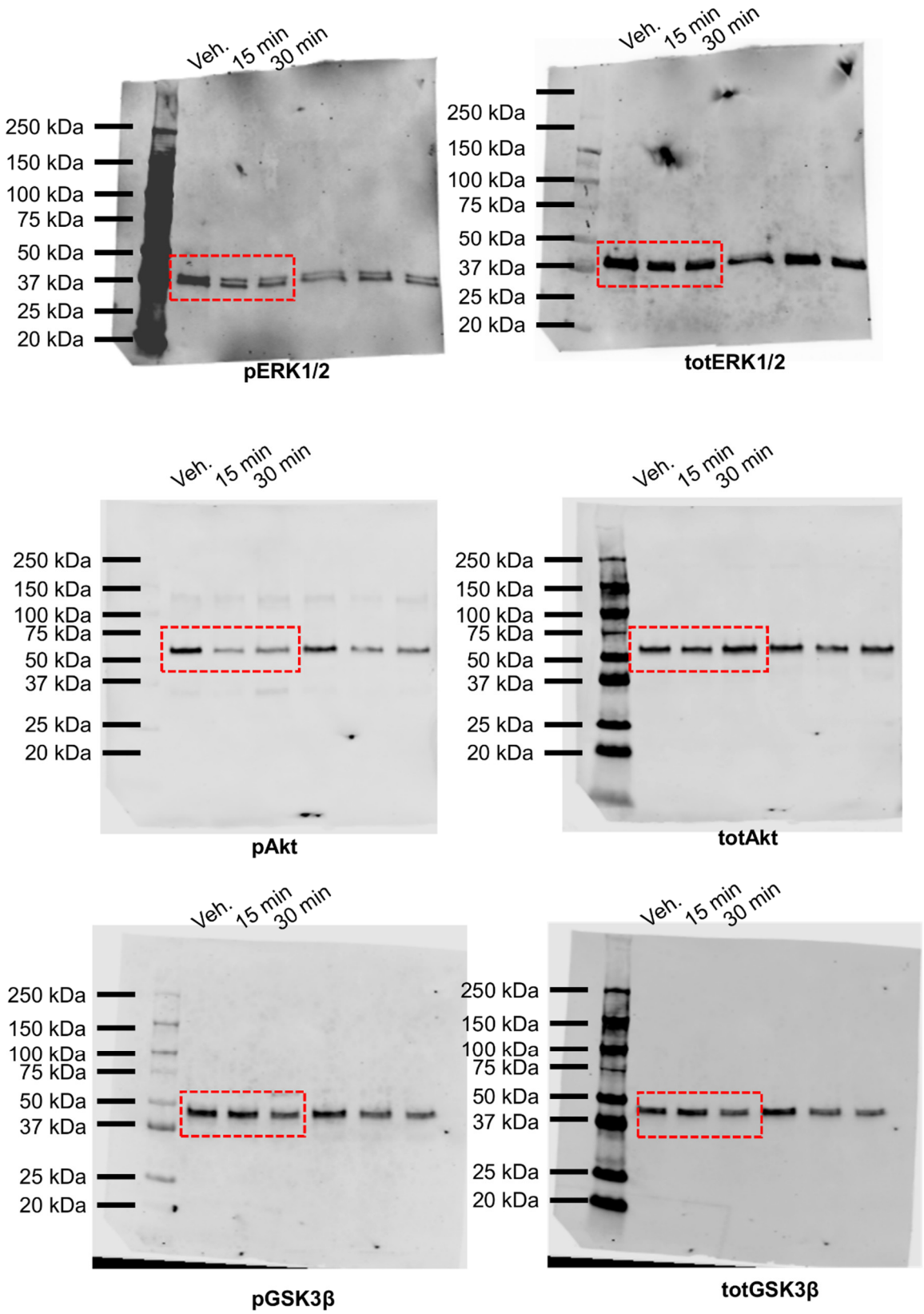

Supplementary Figure 6. Full length blot of western blot shown in main Figure 5 D to F.

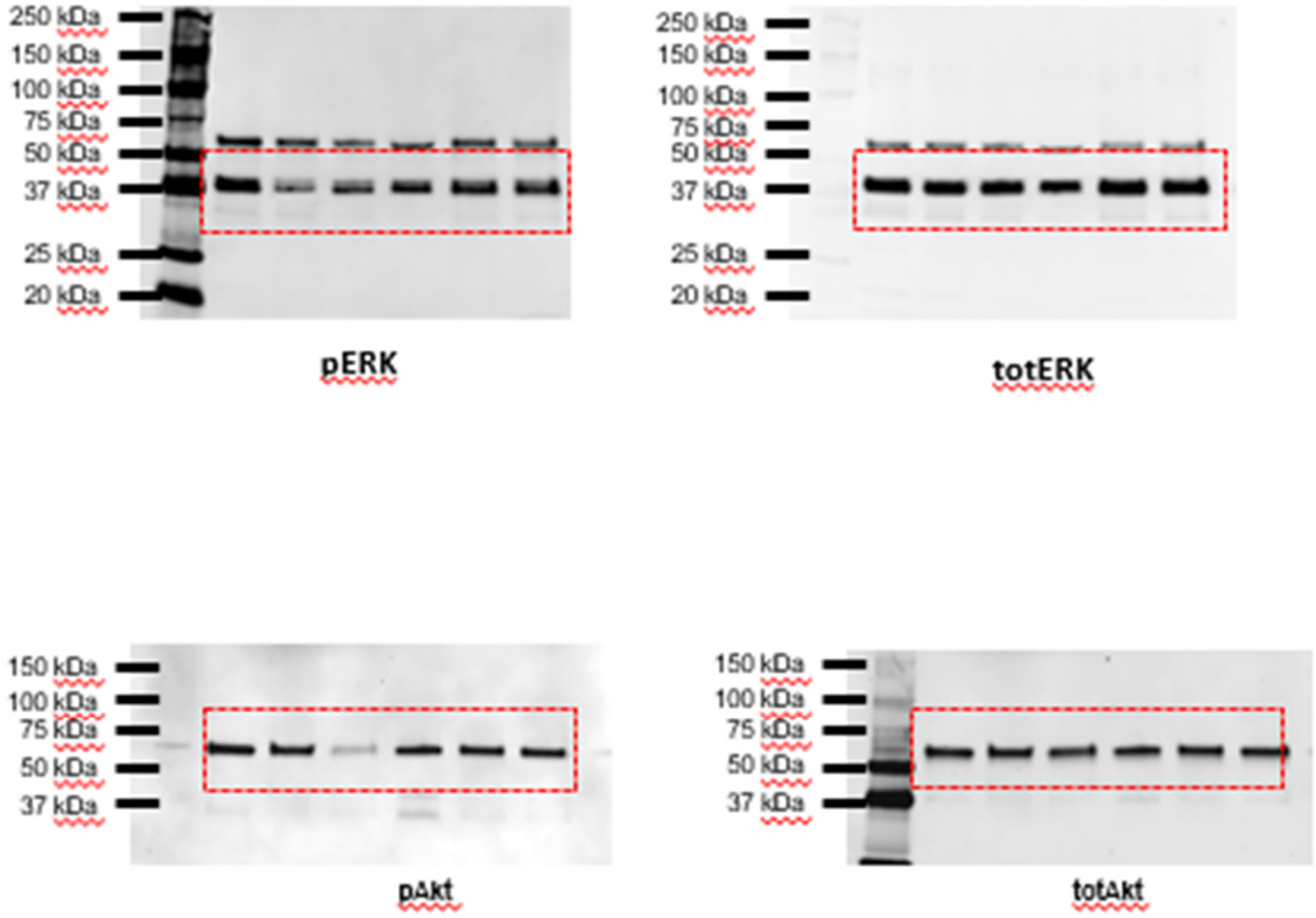

Supplementary Figure 7. Full length blot of western blot shown in main Figure 6A to C.

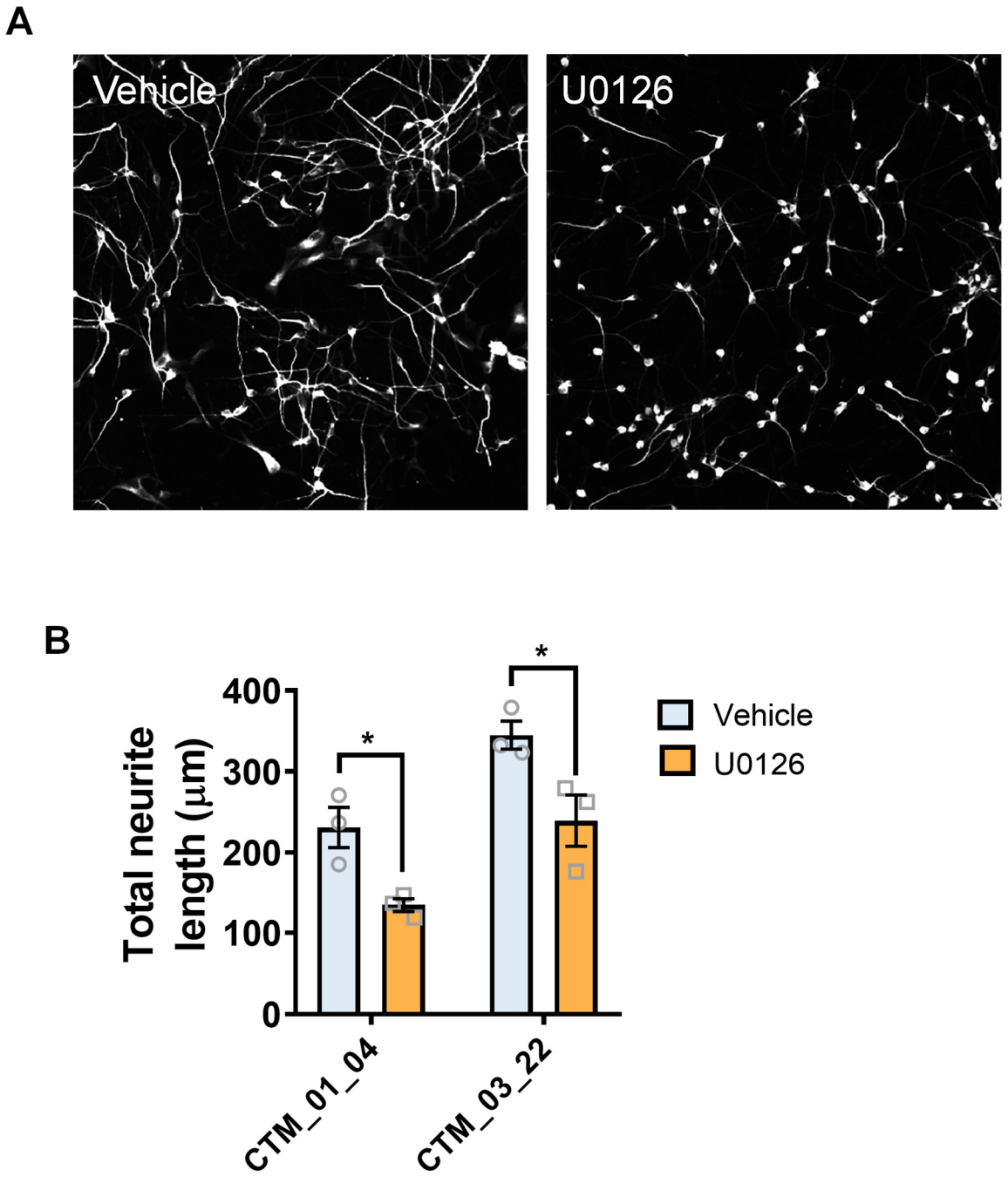

Supplementary Figure 8. (A) Representative images of MAP2 stained day 30 hiPSC-neurons following 24 hour treatment with vehicle or U0126 (10 µM). **(B)** Assessing of total neurite length in all conditions. Data are presented for each individual hiPSC-line: data was generated from 3 independent cultures for each independent hiPSC line.

Treatment with U026 significantly reduced total neurite length compared to vehicle control. Scale bar = 50 μm.